Regulation of NUDT2 expression by estradiol and HER2 in T47D cells

NUDT2 has been suggested a possible estrogen-responsive gene in breast carcinoma cells,[8] but detailed regulatory mechanisms of NUDT2 expression still remain unclear. Therefore, we then examined effects of estradiol on NUDT2 expression in T47D cells. As shown in Figure 5*a*, the level of NUDT2 mRNA expression was dose dependently decreased by estradiol treatment for 3 days, and it became significant from 1 nM compared to the basal level (nontreatment) ($p < 0.05$ and 0.56-fold). Similar significance ($p < 0.01$) was detected when T47D cells were treated with 10 nM estradiol for 1 day under RPMI-1640 without FBS (data not shown). On the other hand, NUDT2 mRNA level did not significantly change when the T47D cells were treated with 5 μM tamoxifen with or without 10 nM estradiol (Fig. 5*a*). The significant suppression of NUDT2 mRNA expression was also detected by the treatment with ERα selective agonist PPT ($p < 0.001$ and 0.5-fold), but not by ERβ selective agonist DPN ($p = 0.81$ and 0.97-fold) (Fig. 5*b*). Estradiol did not significantly change the NUDT2 mRNA expression levels when the T47D cells were treated together with estradiol and a potent ER antagonist ICI 182,780 ($p = 0.23$ and 1.3-fold). Results of immunoblotting analysis also demonstrated that NUDT2 protein level was significantly ($p = 0.02$ and 0.73-fold) decreased by the treatment of 10 nM estradiol for 3 days in T47D cells (Fig. 5*c*). When we performed ChIP assay, ERα was recruited to NUDT2 promoter within 15 min after the addition of 10 nM estradiol, and the promoter occupancy was maximum at 30–45 min after the treatment (Fig. 5*d*).

NUDT2 status was positively associated with HER2 status both in DCIS and IDC tissues (Tables 1 and 2) as demonstrated above. Therefore, these results suggest possible association between NUDT2 and HER2 overexpressions in human breast carcinoma, but such findings have not been reported yet to the best of our best knowledge. Therefore, to examine this hypothesis, we transfected T47D cells with siRNA for HER2 gene. As shown in Figure 5*e*, the level of NUDT2 mRNA was significantly lower in T47D cells transfected with

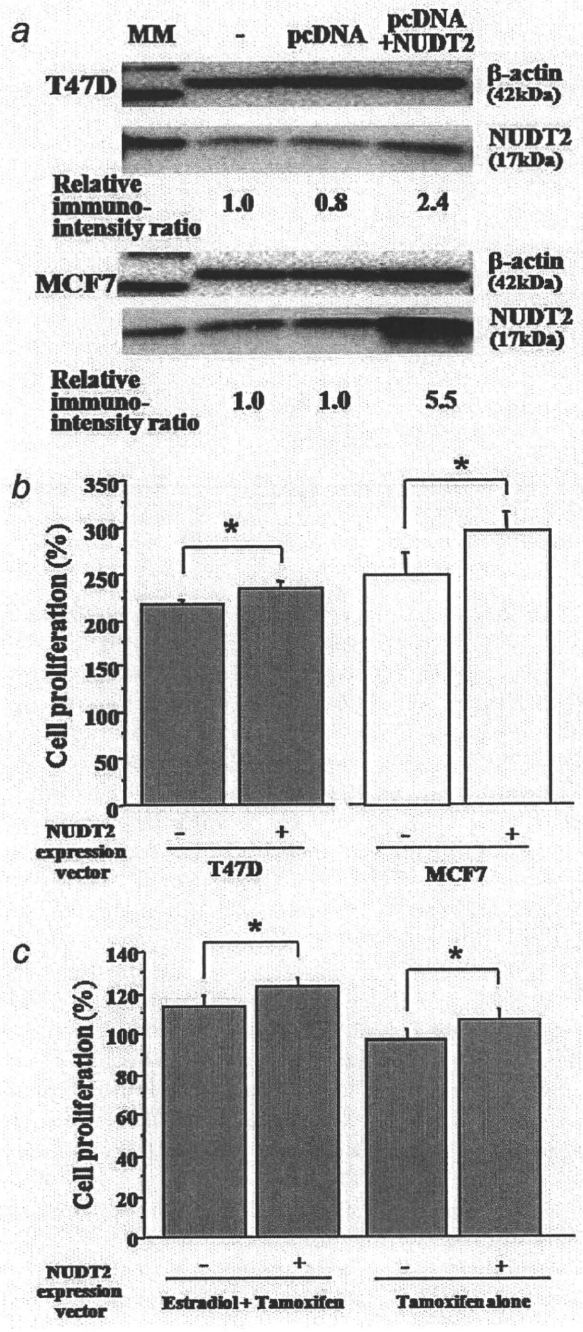

Figure 3. Effects of NUDT2 on the proliferation of breast carcinoma cells by transient transfection. (*a*) Immunoblotting for NUDT2 in T47D and MCF7 cells transfected with NUDT2 expression vector. The protein of cells was extracted at 3 days after the transfection, and 5 μg of protein was loaded in each lane. NUDT2 (lower panel) and β-actin (upper panel) immunoreactivity was detected as a specific band (approximately 17 and 42 kDa, respectively). MM: molecular marker; -: cells without transfection; pcDNA: cells transfected with empty vector (1 μg); pcDNA + NUDT2: cells transfected with NUDT2 expression vector (1 μg). Relative immunointensity ratio of NUDT2 was indicated as a ratio compared to that in the cells without transfection. (*b*, *c*) Proliferation assay of T47D (*b*, *c*) and MCF7 (*b*) cells transfected with NUDT2. After the transfection, the medium was changed to phenol red-free RPMI 1640 medium containing 10% DCC-FBS for 1 day, and these cells were subsequently treated with estradiol (10 nM) and/or tamoxifen (5 μM) for 2 days. The cell number was evaluated as a ratio (%) compared to that at 0 day after the treatment. +: transfection with NUDT2 expression vector; -: transfection with empty vector. Data were presented as mean ± SEM ($n = 4$ independent experiments with three biological replicates), respectively. *$p < 0.05$.

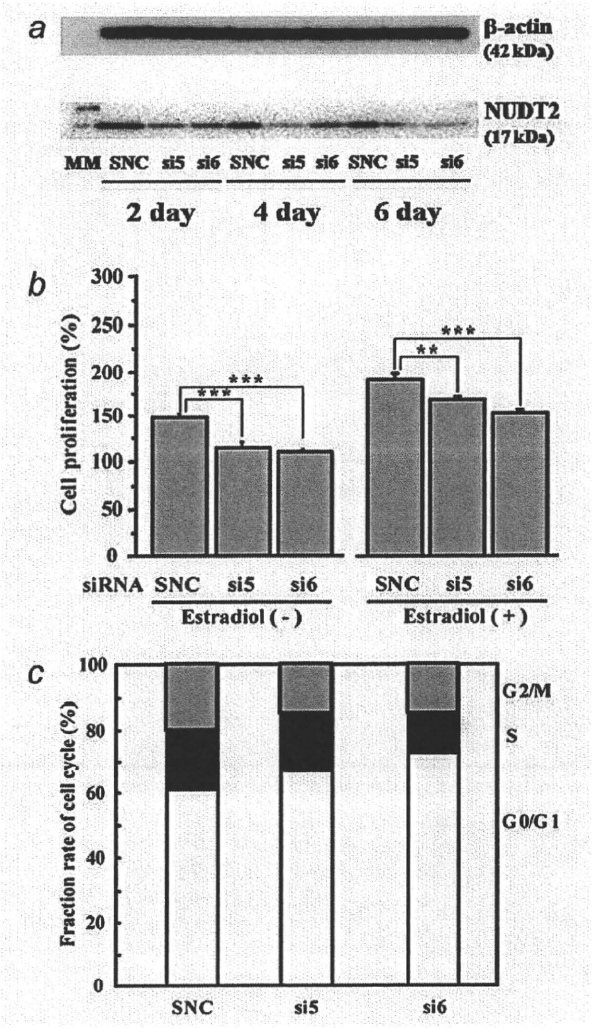

Figure 4. Effects of NUDT2 on the proliferation of T47D cells. (*a*) Immunoblotting for NUDT2 in T47D cells transfected with specific NUDT2 (si5 or si6) siRNA or control (Silencer Negative Control #1; SNC) siRNA. The protein of cells was extracted at 2, 4 or 6 days after the transfection, and 5 μg of protein was loaded in each lane. NUDT2 (lower panel) and β-actin (upper panel) immunoreactivity was detected as a specific band (approximately 17 and 42 kDa, respectively). MM: molecular marker. (*b*) Proliferation assay of T47D cells transfected with si5, si6 or SNC siRNA. After the transfection, the medium was changed to phenol red-free RPMI 1640 medium containing 10% DCC-FBS for 1 day, and the cells were subsequently treated with or without estradiol (10 nM) for 2 days. The cell number was evaluated as a ratio (%) compared to that at 0 day after the treatment. Data were presented as mean ± SEM ($n = 4$ independent experiments with three biological replicates), respectively. $^{**}p < 0.01$ and $^{***}p < 0.001$. (*c*) Flow cytometry analysis in T47D cells transfected with si5, si6 or SNC siRNA. Cell cycle fractions were shown as follows: G0/G1 phase: open bar; S phase: closed bar; G2/M phase: gray bar.

HER2 siRNA than that transfected with SNC siRNA ($p < 0.01$ and 0.30-fold in si3 and $p < 0.05$ and 0.40-fold in si4). However, HER2 mRNA level itself was not significantly ($p = 0.92$) different between the T47D cells treated with NUDT2 (si5 and si6) and SNC siRNA.

Discussion

In this study, we demonstrated that the level of NUDT2 mRNA was significantly higher in DCIS or IDC than non-neoplastic breast tissues. In addition, NUDT2 immunoreactivity was detected in carcinoma cells in 78% of DCIS and 63% of IDC cases, although NUDT2 immunoreactivity was almost negligible in morphologically normal mammary glands. The relatively wide distribution of NUDT2 detected in human breast carcinoma therefore suggests an important role of NUDT2 in human breast carcinoma.

In our study, NUDT2 status evaluated by immunohistochemistry was significantly associated with the Van Nuys classification and Ki-67 LI in DCIS, and with clinical stage, lymph node metastasis and histological grade in IDC. The Van Nuys classification has been established as a potent prognostic classification for DCIS,[19] and Ki-67 LI has also been demonstrated to be closely correlated with the S-phase fraction and mitotic index by numerous investigators.[22,23] Results of our study also demonstrated that NUDT2 status was significantly associated with an increased risk of recurrence or worse prognosis in IDC patients, and NUDT2 status was indeed an independent prognostic factor for both recurrence and prognosis following multivariate analyses. Therefore, these results all indicated an involvement of NUDT2 in the progression and/or recurrence of breast carcinoma. The clinical significance of NUDT2 in human breast carcinoma will, however, need to be further verified in a follow-up study on an independent materials.

Subsequent *in vitro* studies demonstrated that T47D cells transfected with siRNA NUDT2 significantly decreased the cell proliferation associated with increased G0/G1 fraction. Previous *in vitro* studies demonstrated that Ap4A is involved in slowing the process of replication during S-phase, which subsequently allows the opportunity of the cells to repair possible DNA damages,[24–26] and Ap4A itself interrupts the cell cycle progression when damages to the genome are detected in the cells.[27,28] Considering the fact that NUDT2 hydrolyses Ap4A, NUDT2 may promote the proliferation of breast carcinoma cells, at least in a part, through a decrement of the intracellular Ap4A level. An increased level of its expression in DCIS compared to that in IDC and non-neoplastic breast tissues suggests that NUDT2 could play a role in the development of carcinoma in the ductal epithelium of mammary glands, but further investigations are required for clarification.

Recently, Bourdeau *et al.* examined genome-wide identification of EREs in human and detected functional ERE at the promoter region of *NUDT2* gene.[7] In addition, Carroll *et al.* reported that NUDT2 mRNA expression was reduced by addition of estrogens in MCF7 breast carcinoma cells by

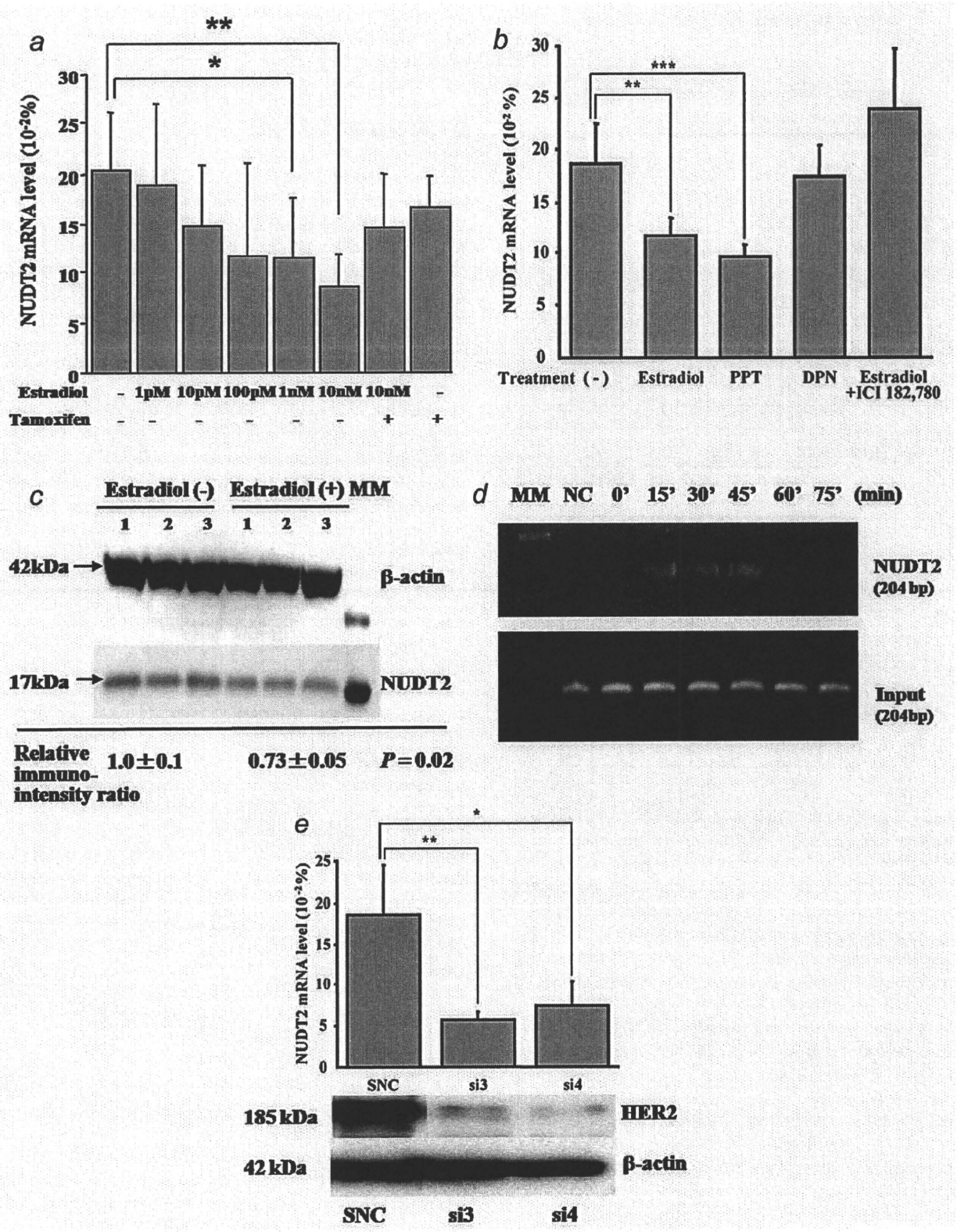
a
**
*
NUDT2 mRNA level (10⁻²%)
30
25
20
15
10
5
0
Estradiol - 1pM 10pM 100pM 1nM 10nM 10nM -
Tamoxifen - - - - - - + +
b
***
**
NUDT2 mRNA level (10⁻²%)
Treatment (-) Estradiol PPT DPN Estradiol +ICI 182,780
c
Estradiol (-) Estradiol (+) MM
1 2 3 1 2 3
42kDa
β-actin
17kDa
NUDT2
Relative immuno-intensity ratio 1.0±0.1 0.73±0.05 P=0.02
d
MM NC 0' 15' 30' 45' 60' 75' (min)
NUDT2 (204 bp)
Input (204bp)
e
*
**
NUDT2 mRNA level (10⁻²%)
SNC si3 si4
185 kDa
HER2
42 kDa
β-actin
SNC si3 si4

genome-wide analysis of ER-binding sites.[8] Therefore, in our study, we also examined possible effects of estrogens on NUDT2 expression. NUDT2 expression was repressed up to half following estradiol in T47D cells through ERα, and subsequent ChIP assay demonstrated binding of ERα with the promoter region of *NUDT2* gene. Results of our study are consistent with those of the previous studies above, and NUDT2 is therefore considered one of estrogen-repressed genes in breast carcinoma cells. Frasor *et al.* demonstrated that a majority (~70%) of estrogen-regulated genes are downregulated, and major functional categories for these estrogen-repressed genes include enzymes, signal transduction and transcription in MCF7 cells.[29] In addition, the estrogen-mediated repression of gene expression was not detected at all in ERα-knockout mice.[30] Therefore, estrogenic functions are characterized not only by estrogen-induced genes but also by estrogen-repressed genes, and therefore, it is important to clarify biological and/or clinical significance of estrogen-repressed genes to understand estrogenic actions in its entirety in human breast carcinoma.

In our study, NUDT2 status was, however, not significantly associated with ER status in DCIS or IDC, although it was expected from the results of our *in vitro* studies described above. Jiang *et al.* reported an induction of NUDT2 expression in human fetal cardiac cells under hypoxic condition.[31] In addition, Yan *et al.* demonstrated that interferon α increased NUDT2 protein level in Huh7 human liver cells.[32] In our study of breast carcinoma patients, NUDT2 status was also positively correlated with HER2 status both in DCIS and IDC cases, and T47D cells transfected with HER2 siRNA significantly decreased the expression level of NUDT2 mRNA. Therefore, several factors other than estrogen may be involved in the regulation of NUDT2 expression in human breast carcinoma cells, which may explain that NUDT2 status was not necessarily associated with ER status in breast carcinomas examined in our study. The *in vitro* experiments conducted in our study are preliminary, and further investigations are required for clarification. However, our experiments may serve as a starting point for clarification of biological functions or regulation mechanisms of NUDT2 in the breast carcinoma.

NUDT2 status was significantly associated with an increased risk of recurrence or worse prognosis in IDC patients in our study, and similar tendency was also detected in ER-positive patients who received tamoxifen therapy as an adjuvant treatment. In addition, results of multivariate analyses demonstrated that NUDT2 status is indeed an independent prognostic factor for both recurrence and overall survival in these patients. Results of our *in vitro* study demonstrated that cell proliferation activity of T47D cells was significantly associated with NUDT2 expression level under the estradiol and/or tamoxifen treatment, and tamoxifen inhibited the estradiol-mediated suppression of NUDT2 expression in these cells. In addition, estrogen-mediated cell proliferation was detected both in NUDT2-positive and -negative T47D cells; the cell proliferation of NUDT2-positive cells without estradiol treatment was nearly equivalent to that of NUDT2-negative cells with estradiol treatment (Fig. 4*b*). However, NUDT2 did not influence the transcriptional activity of ER in T47D cells as results of the luciferase assay demonstrated. All the data above suggest that cell proliferation of breast carcinoma cells is mediated with ER and NUDT2 in different manners or in an additive manner, although the NUDT2 expression was partially suppressed by estradiol, but it awaits for further investigations for clarifying the exact mechanisms. Results of our immunohistochemical studies demonstrated no significant association between NUDT2 status and tumor size in 145 IDC cases (Table 2), but it is true that the tumor size alone does not necessarily represent the overall cell proliferation activity of breast carcinoma,[33] due to the presence

Figure 5. Regulation of NUDT2 expression in T47D cells. (*a*) Effects of estradiol and tamoxifen on NUDT2 mRNA expression level by real-time PCR analysis. T47D cells were cultured with phenol red-free RPMI 1640 medium containing 10% DCC-FBS for 2 days and then treated with indicated concentration of estradiol and/or tamoxifen (5 μM) for 3 days. NUDT2 mRNA level was summarized as the ratio of RPL13A mRNA level (%). Data were presented as mean ± SEM ($n = 4$ independent experiments with three biological replicates), respectively. *$p < 0.05$ and **$p < 0.01$. (*b*) Effects of ER agonists and antagonist on NUDT2 mRNA expression evaluated by real-time PCR analysis. T47D cells were cultured with phenol red-free RPMI 1640 medium containing 10% DCC-FBS for 2 days and then treated with estradiol (10 nM), ERα agonist PPT (10 nM), ERβ agonist DPN (10 nM) or ER antagonist ICI 182,780 (1 μM) for 3 days. Data were presented as mean ± SEM ($n =$ 3 independent experiments with three biological replicates), respectively. **$p < 0.01$ and ***$p < 0.001$. (*c*) Effects of estradiol on NUDT2 protein level by immunoblotting analysis. The cells were cultured with phenol red-free RPMI 1640 medium containing 10% DCC-FBS for 2 days and then treated with or without estradiol (10 nM) for 3 days. A total of 5 μg of protein was loaded in each lane. The results of immunointensity ratio (NUDT2/β-actin) were presented as mean ± SEM ($n = 3$ independent experiments with three biological replicates), and a significant association ($p = 0.02$) was detected between these two groups. (*d*) Recruitment patterns of ERα on NUDT2 promoter in T47D cells treated with estradiol (10 nM) by ChIP assay. The sample before immunoprecipitation by anti-ERα antibody was also used as a control (input; lower panel). MM: molecular marker; NC: negative control sample treated with ethanol. (*e*) Effects of HER2 on NUDT2 mRNA expression by real-time PCR analysis. NUDT2 mRNA level was examined in T47D cells treated with specific HER2 (si3 or si4) or SNC siRNA 3 days after the transfection (upper panel). NUDT2 mRNA level was summarized as the ratio of RPL13A mRNA level (%). Data were presented as mean ± SEM ($n = 3$ independent experiments with three biological replicates), respectively. *$p < 0.05$ and **$p < 0.01$. The knockdown effects mediated by si3 or si4 siRNA were subsequently confirmed by immunoblotting for HER2 3 days after the transfection (lower panels).

of the amount of stromal cells in the tumor tissues. Therefore, residual carcinoma cells after surgical treatment in NUDT2-positive breast carcinomas may still have the potential to rapidly grow regardless of antiestrogen therapies such as tamoxifen, thereby resulting in an increased recurrence and poor prognosis in these patients.

In summary, NUDT2 immunoreactivity was frequently detected in the breast carcinoma in our study. NUDT2 status was significantly associated with an increased risk of recurrence or worse prognosis of IDC patients, and it was an independent prognostic factor. Results of further *in vitro* studies demonstrated that proliferation activity of T47D cells was associated with NUDT2 level according to the treatment of estradiol and/or tamoxifen. These findings suggest that NUDT2 promotes the proliferation of breast carcinoma cells by different mechanisms from estrogens, and the NUDT2 status is established as a potent prognostic factor in human breast carcinomas.

Acknowledgements

The authors appreciate the skillful technical assistance of Ms. Miki Mori and Mr. Katsuhiko Ono (Department of Pathology, Tohoku University Graduate School of Medicine).

References

1. McLennan AG. The Nudix hydrolase superfamily. *Cell Mol Life Sci* 2006;63: 123–43.
2. Nishimura A. The timing of cell division: Ap4A as a signal. *Trends Biochem Sci* 1998; 23:157–9.
3. Segal E, Le Pecq JB. Relationship between cellular diadenosine 5′,5‴-P1,P4-tetraphosphate level, cell density, cell growth stimulation and toxic stresses. *Exp Cell Res* 1986;167:119–26.
4. Vartanian AA, Suzuki H, Poletaev AI. The involvement of diadenosine 5′,5‴-P1,P4-tetraphosphate in cell cycle arrest and regulation of apoptosis. *Biochem Pharmacol* 2003:65:227–35.
5. Rotllan P, Rodriguez-Perrer CR, Maeso MC, Oaknin S. Expression of diadenosine tetraphosphatase and diadenosine triphosphatase in human tumours: A preliminary investigation. Program of the 7th International Symposium on Predictive Oncology & Intervention Strategies 2004; 28:S90–S91 (Abstract 137).
6. Rapaport E, Zamecnik PC. Presence of diadenosine 5′,5‴-P1, P4-tetraphosphate (Ap4A) in mamalian cells in levels varying widely with proliferative activity of the tissue: a possible positive "pleiotypic activator". *Proc Natl Acad Sci USA* 1976; 73:3984–8.
7. Bourdeau V, Deschênes J, Métivier R, Nagai Y, Nguyen D, Bretschneider N, Gannon F, White JH, Mader S. Genome-wide identification of high-affinity estrogen response elements in human and mouse. *Mol Endocrinol* 2004;18:1411–27.
8. Carroll JS, Meyer CA, Song J, Li W, Geistlinger TR, Eeckhoute J, Brodsky AS, Keeton EK, Fertuck KC, Hall GF. Genome-wide analysis of estrogen receptor binding sites. *Nat Genet* 2006;38:1289–97.
9. Moon HG, Han W, Noh DY. Underweight and breast cancer recurrence and death: a report from the Korean Breast Cancer Society. *J Clin Oncol* 2009;27: 5899–905.
10. Suzuki T, Miki Y, Moriya T, Akahira J, Ishida T, Hirakawa H, Yamaguchi Y, Hayashi S, Sasano H. 5a-Reductase type 1 and aromatase in breast carcinoma as regulators of in situ androgen production. *Int J Cancer* 2007;120:285–91.
11. Allred DC, Harvey JM, Berardo M, Clark GM. Prognostic and predictive factors in breast cancer by immunohistochemical analysis. *Mod Pathol* 1998;11:155–68.
12. Dumoulin FL, Nischalke HD, Leifeld L, von dem Bussche A, Rockstroh JK, Sauerbruch T, Spengler U. Semi-quantification of human C-C chemokine mRNAs with reverse transcription/real-time PCR using multi-specific standards. *J Immunol Methods* 2000;241:109–19.
13. Gottfried-Blackmore A, Croft G, McEwen BS, Bulloch K. Transcriptional activity of estrogen receptors ERα and ERβ in the EtC.1 cerebellar granule cell line. *Brain Res* 2007;1186:41–7.
14. Howell A, Osborne CK, Morris C, Wakeling AE. ICI 182,780 (Faslodex): development of a novel, "pure" antiestrogen. *Cancer* 2000;89:817–25.
15. Niikawa H, Suzuki T, Miki Y, Suzuki S, Nagasaki S, Akahira J, Honma S, Evans DB, Hayashi S, Kondo T, Sasano H. Intratumoral estrogens and estrogen receptors in human non-small cell lung carcinoma. *Clin Cancer Res* 2008;14: 4417–26.
16. Suzuki T, Inoue A, Miki Y, Moriya T, Akahira J, Ishida T, Hirakawa H, Yamaguchi Y, Hayashi S, Sasano H. Early growth responsive gene 3 in human breast carcinoma: a regulator of estrogen-meditated invasion and a potent prognostic factor. *Endocr Relat Cancer* 2007; 14:279–92.
17. Aoki S, Cho SH, Ono M, Kuwano T, Nakao T, Kuwano M, Nakagawa S, Gao JQ, Mayumi T, Shibuya M, Kobayashi M. Bastadin 6, a spongean brominated tyrosine derivative, inhibits tumor angiogenesis by inducing selective apoptosis to endothelial cells. *Anticancer Drugs* 2006;17:269–78.
18. Shang Y, Hu X, DiRenzo J, Lazar MA, Brown M. Cofactor dynamics and sufficiency in estrogen receptor-regulated transcription. *Cell* 2000;103: 843–52.
19. Silverstein MJ, Poller DN, Waisman JR, Colburn WJ, Barth A, Gierson ED, Lewinsky B, Gamagami P, Slamon DJ. Prognostic classification of breast ductal carcinoma-in-situ. *Lancet* 1995;345: 1154–7.
20. Elston CW, Ellis IO. Pathological prognostic factors in breast cancer. I. The value of histological grade in breast cancer: experience from a large study with long-term follow-up. *Histopathology* 1991;19: 403–10.
21. Park K, Han S, Kim HJ, Kim J, Shin E. HER2 status in pure ductal carcinoma in situ and in the intraductal and invasive components of invasive ductal carcinoma determined by fluorescence in situ hybridization and immunohistochemistry. *Histopathology* 2006;48:702–7.
22. Weidner N, Moore DH, II, Vartanian R. Correlation of Ki-67 antigen expression with mitotic figure index and tumor grade in breast carcinomas using the novel "paraffin"-reactive MIB1 antibody. *Hum Pathol* 1994;25:337–42.
23. MacGrogan G, Jollet I, Huet S, Sierankowski G, Picot V, Bonichon F, Coindre JM. Comparison of quantitative and semiquantitative methods of assessing MIB-1 with the S-phase fraction in breast carcinoma. *Mod Pathol* 1997;10: 769–76.
24. Varshavsky A. Diadenosine 5′,5‴-P1, P4-tetraphosphate: a pleiotropically acting alarmone? *Cell* 1983;34:711–12.
25. Varshavsky A. Do stalled replication forks synthesize an alarmone? *J Theor Biol* 1983; 105:704–14.
26. Baker JC, Smale ST, Tjian R, Ames BN. Inhibition of simian virus 40 DNA replication in vitro by poly(ADP-ribosyl)ated diadenosine tetraphosphate. *J Biol Chem* 1987;262:14855–8.
27. Elledge SJ. Cell cycle checkpoints: preventing an identity crisis. *Science* 1996; 274:1664–72.

28. Paulovich AG, Toczyski DP, Hartwell LH. When checkpoints fail. *Cell* 1997;88: 315–21.
29. Frasor J, Danes JM, Komm B, Chang KC, Lyttle CR, Katzenellenbogen BS. Profiling of estrogen up- and down-regulated gene expression in human breast cancer cells: insights into gene networks and pathways underlying estrogenic control of proliferation and cell phenotype. *Endocrinology* 2003;144: 4562–74.
30. Hewitt SC, Deroo BJ, Hansen K, Collins J, Grissom S, Afshari CA, Korach KS. Estrogen receptor-dependent genomic responses in the uterus mirror the biphasic physiological response to estrogen. *Mol Endocrinol* 2003;17:2070–83.
31. Jiang C, Lu H, Vincent KA, Shankara S, Belanger AJ, Cheng SH, Akita GY, Kelly RA, Goldberg MA, Gregory RJ. Gene expression profiles in human cardiac cells subjected to hypoxia or expressing a hybrid form of HIF-1 alpha. *Physiol Genomics* 2002;8:23–32.
32. Yan W, Lee H, Yi EC, Reiss D, Shannon P, Kwieciszewski BK, Coito C, Li XJ, Keller A, Eng J, Galitski T, Goodlett DR, et al. System-based proteomic analysis of the interferon response in human liver cells. *Genome Biol* 2004;5:R54.
33. Stumpp J, Dietl J, Simon W, Geppert M. Growth fraction in breast carcinoma determined by Ki-67 immunostaining: correlation with pathological and clinical variables. *Gynecol Obstet Invest* 1992;33: 47–50.

JJCO Japanese Journal of Clinical Oncology

Original Articles

Jpn J Clin Oncol 2010;40(10)905–912
doi:10.1093/jjco/hyq070
Advance Access Publication 21 May 2010

The Correlation Between Ultrasonographic Findings and Pathologic Features in Breast Disorders

Kentaro Tamaki[1,2,3,*], Hironobu Sasano[2], Takanori Ishida[1], Kazuyuki Ishida[2], Minoru Miyashita[1], Motohiro Takeda[1], Masakazu Amari[1], Narumi Harada-Shoji[1], Masaaki Kawai[1], Toshiyuki Hayase[4], Nobumitsu Tamaki[3] and Noriaki Ohuchi[1]

[1]Department of Surgical Oncology, Tohoku University Graduate School of Medicine, [2]Department of Pathology, Tohoku University Hospital, Sendai, Miyagi, [3]Department of Breast Surgery, Nahanishi Clinic, Naha, Okinawa and [4]Institute of Fluid Science, Tohoku University, Sendai, Miyagi, Japan

*For reprints and all correspondence: Kentaro Tamaki, Department of Surgical Oncology, Tohoku University Graduate School of Medicine, 1-1 Seiryo-machi, Aoba-ku, Sendai, Miyagi 980-8574, Japan.
E-mail nahanisikenta@yahoo.co.jp

Received January 9, 2010; accepted April 7, 2010

Downloaded from jjco.oxfordjournals.org at Tohoku University on May 6, 2011

Objective: Breast ultrasonography has gained widespread acceptance as a diagnostic tool for the evaluation of human breast disorders. It is important to evaluate the correlation of ultrasonography findings with the corresponding histopathological features.
Method: We retrospectively reviewed the 154 cases of breast disorders. We evaluated the correlation the ultrasonography findings and carcinoma cells extension with their corresponding histopathological findings. In addition, we also studied the information on estimation of histological types and cancer extension used by the other modalities such as computed tomography and magnetic resonance imaging.
Results: The concordance rate for margins between ultrasonography findings and histopathological features was 91.6% ($P < 0.001$) and that for boundary zone was 87.0% ($P < 0.001$). Histopathological correlation of internal and posterior echoes demonstrated that internal low echo masses were composed of fibroblastic cells with marked collagenization in the stroma, or the cases in which carcinoma cells proliferated in a monotonous, solid and/or expanding manners. Attenuation of posterior echo was detected in the cases associated with hyperplasia of collagenized fibroblastic stroma. An increased cellularity in the mass with prominent large tumor nests and little fibrous stroma demonstrated the accentuation or no alterations of the posterior echo. The concordance rate of borders was 84.4% ($P < 0.001$). The correlation between estimated histological type by ultrasonography diagnosis and actual histological types was 87.0%. An overall detection rate of carcinoma extension by ultrasonography was 86.4%. In addition, an overall detection rate of carcinoma extension by ultrasonography, magnetic resonance imaging and computed tomography was 93.8%.
Conclusion: These results demonstrated correlation between histopathological and ultrasonographic findings of the breast lesions is cardinal for quality control or improving the quality of ultrasonography.

Key words: breast ultrasound – histopathologic findings – carcinoma extension

INTRODUCTION

Breast cancer has become one of the leading causes of death among women. Early clinical detection of breast cancer through screening has led to the detection of the tumor at a relatively earlier clinical stage, which definitely reduced its mortality. The mammographic appearance of breast carcinoma has been well known to vary greatly (1). On the other

© The Author (2010). Published by Oxford University Press. All rights reserved.

hand, breast ultrasonography (US) has gained widespread acceptance as a diagnostic tool for the evaluation of breast disorders (2). It is true that some breast diseases that are obscured by dense breast tissue at mammography can be detected with US. US has been in general proposed to serve better in the detection of breast cancer if the patient is young or the masses are small (3,4). Results of many previously published studies have demonstrated the diagnostic benefits in differentiating benign from malignant breast disease in the evaluation using US (5). It was well known that carcinomas are classically described as irregular solid masses with a heterogenous texture and reduced sound transmission in the US, resulting in what is called 'shadowing' behind the lesion (5,6). In addition, a vertical orientation of the lesion is described more often in breast carcinoma in US evaluation (5,6). It is also true that not all carcinomas fulfill these criteria and some do only partially (5). In general, an accurate correlation of US findings with their corresponding histopathologic features is considered most important in US evaluation in this setting.

Breast-conserving surgery is being widely applied in the treatment of early breast cancer. In order to perform conserving surgery, it is very important to detect carcinoma extension and determine the excision area as accurately as possible in the preoperative setting for the benefits of the patients (7,8). Complete removal of a breast tumor with tumor-negative surgical margins is considered most important for avoiding local recurrence in breast-conserving surgery. With high-resolution equipment available, US can detect smaller non-palpable cancers not necessarily detected on high-quality mammography. Excellent visualization of extended intraductal component has been reported using US in some institutions (9,10). However, few have demonstrated the limitation of the US to detect small lesions. Therefore, we attempted to evaluate carcinoma infiltration based on US findings, through revealing histopathologic features of the carcinoma cells infiltration which cannot be detected by US. In addition, in order to overcome these possible limitations, magnetic resonance imaging (MRI) and computed tomography (CT) are being increasingly utilized for the preoperative evaluation of carcinoma extension (11–13). Therefore, we also evaluated the information regarding the detection of cancer infiltration by US in conjunction with MRI and CT.

It is very important to evaluate the correlation of US findings with the corresponding histopathological features. The purpose of this study is therefore, to evaluate the correlation of the US findings including shape, boundary zone, internal and posterior echo, anterior and posterior borders, estimated histological types and carcinoma infiltration with their corresponding histopathological findings of the same lesions. In particular, for internal and posterior echoes, attenuation has been considered to be provided by a highly cellular fibroblastic proliferation (2,14). However, none has ever reported that internal and posterior echo were indeed based on the ratio of intratumoral carcinoma cells and fibroblastic stroma, and histological stromal characteristics of the same lesions. We therefore indicated that anterior and posterior echoes were indeed caused by the ratio of intratumoral carcinoma cells and fibroblastic stroma, and histological stromal characteristics. In addition, some histological types demonstrated low concordance rates between estimated or the histological types estimated by ultrasonographic findings and actual histological types. Therefore, we also discussed this particular discordance between estimated US findings and histologic types, in detail.

Table 1. Histological types of examined cases

Histological types (all)	154
Invasive ductal carcinoma (IDC)	132
Ductal carcinoma in situ (DCIS)	7
Invasive lobular carcinoma (ILC)	10
Mucinous carcinoma	5

PATIENTS AND METHODS

Patients

We retrospectively reviewed the US findings and the histopathologic features of 154 breast lesions for which surgery was performed in Tohoku University Hospital from 1 January 2006 to 31 December 2007 and in which the patients were initially detected by US. The cases treated with neo-adjuvant chemotherapy were excluded from this study of correlating preoperative US findings with histopathlogical analyses. We received informed consents from the patients and the protocol for this study was approved by the Ethics Committee at Tohoku University School of Medicine. The median age of the patients was 57 years (range, 27–85). Of the remaining consecutive 154 patients, 132 were diagnosed histopathologically as invasive ductal carcinomas (IDC), 7 with ductal carcinoma in situ (DCIS), 10 with invasive lobular carcinomas (ILC) and 5 with mucinous carcinomas (Table 1).

US and Histopathologic Analyses

The US were assessed by one of experienced eight breast surgeons of Tohoku University Hospital. They got the consensus meeting of US for a week to standardize the US exam. In addition, two surgical oncologists independently evaluated the US findings in a retrospective manner, without the knowledge of subsequent histopathological diagnosis. These two investigators were also blinded to the clinical outcome of the patients. The US examination was carried out using the following mechanical scanners: Aloka SSD 3500 (Aloka Co., Tokyo, Japan) with a 10-MHz transducer.

Surgical specimens had been fixed in 10% formaldehyde solution and cut into serial 5-mm thick slices. Histopathological slides in each tumor were reviewed by two pathologists independently without knowledge of the breast US findings. They used Olympus (Tokyo, Japan) BX50 and 20X objectives for the analysis.

Downloaded from jjco.oxfordjournals.org at Tohoku University on May 6, 2011

Of two or more hardcopy transverse and sagittal plane images of breast lesions, only the largest lesion was analyzed in this study. In the patients with multiple breast lesions, only the largest lesion was evaluated. US findings were subsequently analyzed according to the American College of Radiology Breast Imaging Reporting and Data System (BI-RADS) sonographic classification (2) and the Japan Association of Breast and Thyroid Sonology (JABTS) breast sonographic classification (14). The presence of a mass, margin, boundary zone, internal echoes, posterior echoes and associated findings were each recorded. Histopathological evaluations were based on the Japanese Breast Cancer Society (2008) (15), World Health Organization (WHO) histological classification of tumors of the breast (1) and Rosen's Breast Pathology (16). (i) Margin was tentatively classified into circumscribed or not and also histopathologically classified into these two categories above. (ii) For boundary zone, we analyzed the presence or absence of halo in US. Ultrasonographic 'Halo' corresponded to the histopathologic features in which carcinoma cells invade into fat tissue admixed with adipocytes and elastic fiber (14). We termed the histopathologic feature 'histopathologic halo' and evaluated the existence of the 'histopathologic halo' (Fig. 1). (iii) Internal echo was tentatively classified into low and equal/heterogenous, and posterior echo was tentatively classified into accentuating, no change and attenuating (14). Histopathologic features corresponding to internal and posterior echoic findings were defined by the ratio of carcinoma cells to stroma and the following characteristics related to stromal architecture; collagenization or poor collagenization. We analyzed the intratumoral stroma in five representative fields per case (×200) (Fig. 2). (iv) We analyzed relevant findings about interruption of the anterior and posterior borders of the mammary gland. Interruption of the borders demonstrated extension in adipose tissue, whereas non-interruption demonstrated extension in gland (Fig. 3). (v) We examined the concordance between the estimated and actual histological types. We estimated histological types as followings; IDC, DCIS, ILC and mucinous carcinoma by US without knowledge of histopathological diagnoses.

US, CT and MRI were performed prior to breast-conserving surgery. A 16-row detector CT system (Somatom Sensation Cardiac; Siemens Medical Solution, Erlangen, Germany) was used with CT skin marker, consisting of a paper seal and seven 75-mm non-lead lines with an open window between each line, over the location of the target (13). The breast MRI was obtained using a 1.5 tesla MRI clinical scanner (Magnetom Vision, Siemens, Erlangen, Geramany) (17). The histopathologic diagnosis and the carcinoma extension in all slices were determined by the two pathologists. The surgical margin was defined as positive margin when there were malignant cells at the surgical margin and within 5 mm of the surgical margin. The accurate ratio between the cancer extension detected by the US and the histopathologic cancer extension was evaluated. We also studied the information on detecting cancer extension used by the other modalities such as CT and MRI. In addition, the histopathological characteristics of the cases which could not to be detected by the US were also evaluated. If there were discrepancies of carcinoma extension and estimated histological types among these modalities, we returned to examine the discrepant lesions by US again. When the US findings of the lesions represented desmoplastic change or stromal reaction, we accepted the diagnoses by MRI and CT. On the other hand, when the US findings represented normal variations, we accepted the US diagnoses.

Statistically analysis, such as the one-factor ANOVA and simple regression analysis, were performed using StatMate III for Windows ver. 3.18 (ATMS, Tokyo, Japan). The results were considered significant at $P < 0.05$.

RESULTS

Evaluation of the Margins of the Lesion

Twenty-six out of the 154 were circumscribed masses. Of the 26 circumscribed tumors detected by US, 18 cases

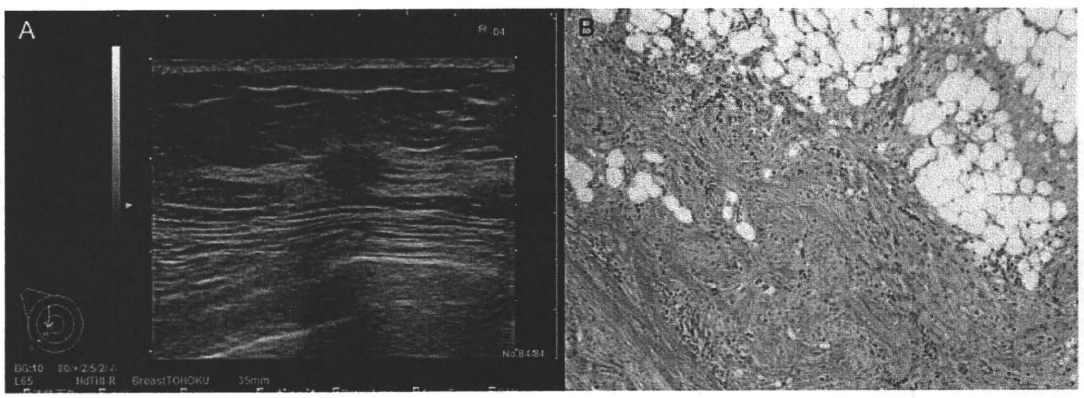

Figure 1. Representative illustrations of 'halo'. (A) 'Halo' of the US finding. (B) The histopathologic feature representing infiltration of carcinoma cells into the surrounding tissues, such as fat tissue and elastic fiber.

Downloaded from jjco.oxfordjournals.org at Tohoku University on May 6, 2011

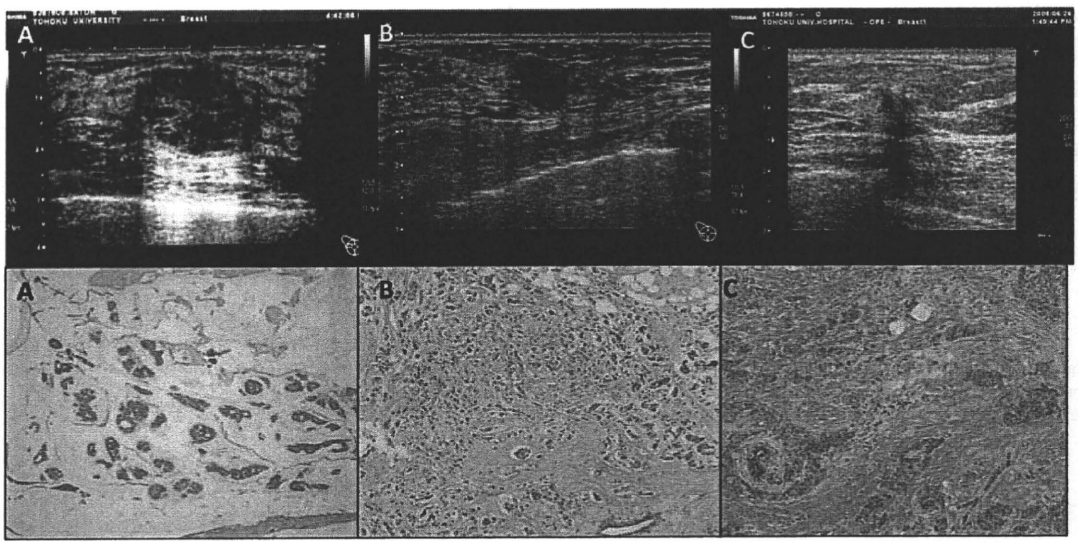

Figure 2. Representative illustrations of internal echoe and posterior echoe. (A) Shows internal echo is heterogenous and posterior echo is accentuating. The histologic type is mucinous carcinoma in which intratumoral structure is heterogenous and constructed by mucin. (B) Shows internal echo is low or hetrogenous and posterior echo is no change. The intratumoral histopathologic feature is heterogenous and poor collagenized stroma. Whereas (C) shows internal echo is low and posterior echo is attenuation. The intratumoral histopathologic feature is heterogenous but the stroma is marked collagenized.

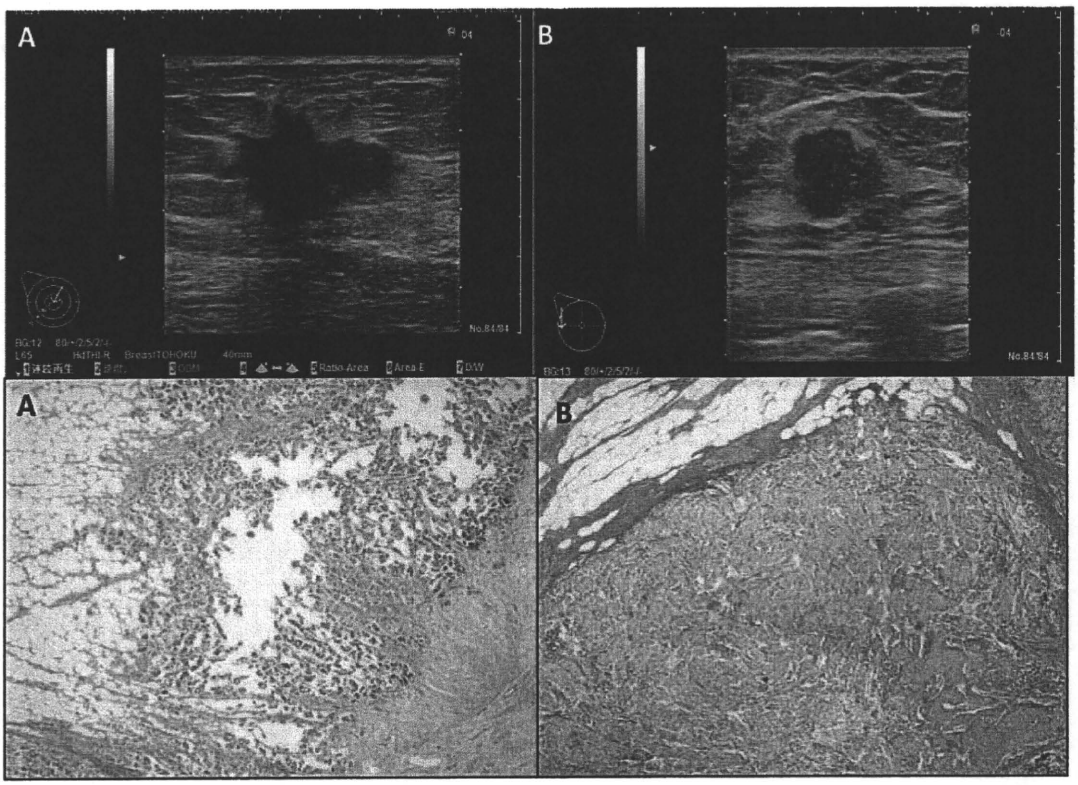

Figure 3. Representative illustrations of interruption and not interruption of the mammary borders. (A) Shows interruption of the anterior border. Histopathologically, carcinoma cells extend to fat. (B) Shows not interruption of the borders. Histopathologically, carcinoma cells extend in the mammary gland.

(69.2%) were also histopathologically circumscribed. Not circumscribed masses were 128 tumors in our present study. One hundred and sixteen out of these 128 tumors (90.6%) were also histopathologically 'not circumscribed'. The rate of concordance between US and histopathological findings was 87.0% ($P < 0.001$).

Downloaded from jjco.oxfordjournals.org at Tohoku University on May 6, 2011

Boundary Zone (Halo)

Eighty-nine out of these154 tumors were recognized with halo using US. Seventy-eight out of these 89 tumors with halo were defined as 'histopathologic halo' (Table 2). The rate of concordance was 87.6%. Sixty-five out of the 154 tumors turned out to be the masses without halo. Fifty-six out of the 65 non-halo tumors (86.2%) were also non-histopathologic halo tumors. The rate of concordance for boundary zone between US and histopathologic findings was 87.0% ($P < 0.001$).

Table 2. US findings, the number of cases and the ratio of accuracy between US findings and histopathological features, of margin, boundary zone and associated findings

US findings	No. of cases	Rate of concordance (%)
Margin		
Circumscribed	26	69.2
Not circumscribed	128	90.6
Boundary zone (halo)		
halo (+)	89	87.6
halo (−)	65	86.2
Associated findings (Interruption of the mammary borders)		
Interruption	112	83.0
Non-interruption	42	88.1

Internal and Posterior Echoes

About 59.7% of the tumors in which internal echoes were equal/heterogeneous histopathologically were associated with poor collagenized stroma and heterogenous intratumoral structure (the ratio of carcinoma cells to stroma was 3:1–1:3) (Fig. 4A). However, tumors associated with low echo levels demonstrated marked collagenized stroma and the higher fibroblastic stromal ratio. As for posterior echo, accentuating tumors histopathologically demonstrated carcinoma cells proliferated in pushing, encapsuled and monotonous fashions, and were also demonstrated in all mucinous carcinoma examined. About 76.1% of the tumors classified as 'no changes' also demonstrated the patterns of marked intratumoral heterogeneity. In addition, ulrtasonographically attenuating cases (43 out of the 153 tumors, 28.1%) were associated with marked collagenized stroma and higher fibroblastic stromal ratio (Fig. 4B).

Histopathological Correlations with Other Ultrasonographic Findings (Interruption of the Anterior Or Posterior Borders of the Mammary Gland)

Interruption of anterior and posterior borders tumors were detected in 112 out of the 153 tumors. Ninety-three out of the 112 tumors (83.0%) were also histopathologically interpreted as extension into adipose tissue. Non-interruption tumors were seen in 42 cases. Thirty-seven out of the

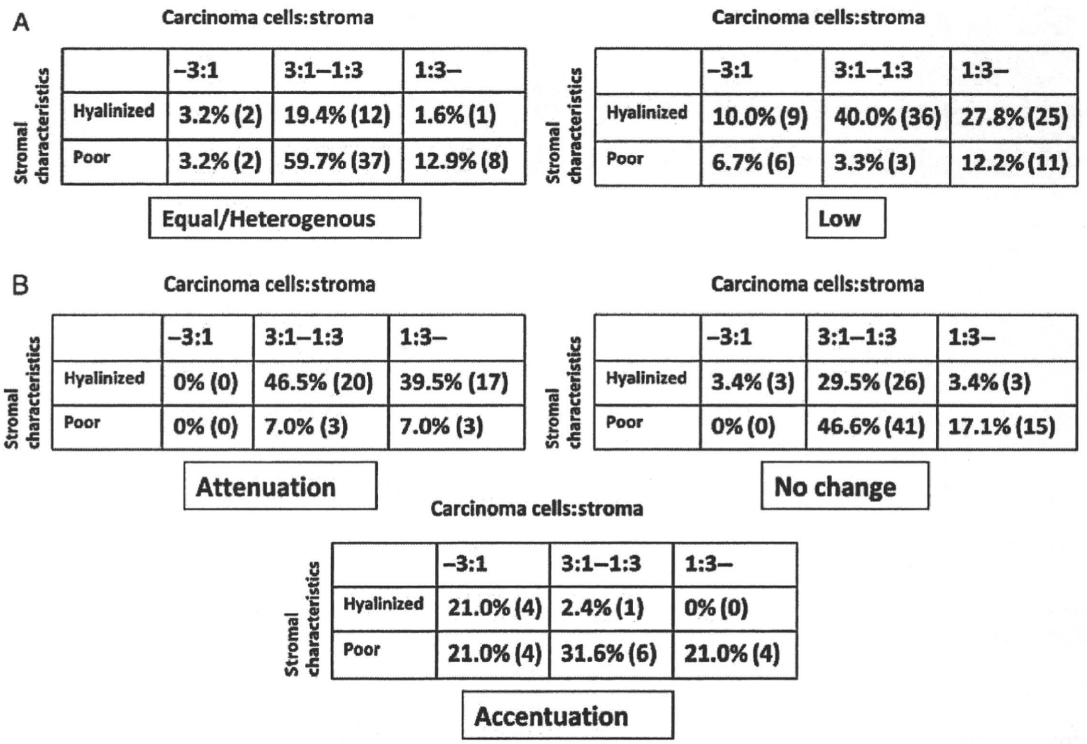

Figure 4. Analysis of internal echoes and posterior echoes according to the ratio of carcinoma cells to stroma and the stromal characteristics. (A) Is the results of internal echo and (B) is the results of posterior echoes.

Downloaded from jjco.oxfordjournals.org at Tohoku University on May 6, 2011

42 tumors (88.1%) were histopathologically infiltration in mammary gland or non-invasive carcinomas. The rate of concordance of these borders was 84.4% ($P < 0.001$).

The Correlation Between Final Us and Histopathological Diagnoses

The ratio of the correlation between estimated histological types by US diagnosis and histopathological types was 91.6% (141 out of the 154 tumors). The concordance rates between US findings and the following histologic types; IDC, DCIS, ILC and mucinous carcinoma were 98.5% (130 out of the 132 tumors), 14.3% (1 out of the 7 tumors), 60.0% (6 out of the 10 tumors) and 80.0% (4 out of the 5 tumors), respectively (Table 3). US was limited in its ability to detect the lesions with <1 mm in diameter. The concordance rate of combined modalities was 96.1% (148 of 154 tumors) with US, CT with CT skin marker and MRI; IDC, DCIS, ILC and mucinous carcinoma were 99.2% (131 out of the 132 tumors), 57.1% (4 out of the 7 tumors), 80.0% (8 out of the 10 tumors) and 100% (5 out of 5 tumors), respectively.

Table 3. The concordance rates between US diagnosis and the histological types

Histological types	Concordance	Not concordance	Rate of concordance (%)
IDC	130	2	98.5
DCIS	1	6	14.3
ILC	6	4	60.0
Mucinous	4	1	80.0

Correlation Between Ultrasonographic and Histopathological Carcinoma Extension

The overall detection rate of carcinoma extension by US was 86.4% (133 out of the 154 tumors). Seventeen out of the 21 tumors (81%) in which US could not detect carcinoma extension demonstrated low-grade intraductal components (Fig. 5A and B), and these lesions were also <1 mm in diameter. Three out of these 21 cases turned out to be invasive ILC in which carcinoma cells invaded with forming single cell pattern (Fig. 5C) and small LCIS extension (Fig. 5D). One was the infiltrated lesion of IDC. This tumor was invaded with forming single cell pattern with poor stromal reaction, similar to ILC. The detection rate of combined modalities was 93.8% (144 of 154 tumors) with US, CT with CT skin marker and MRI.

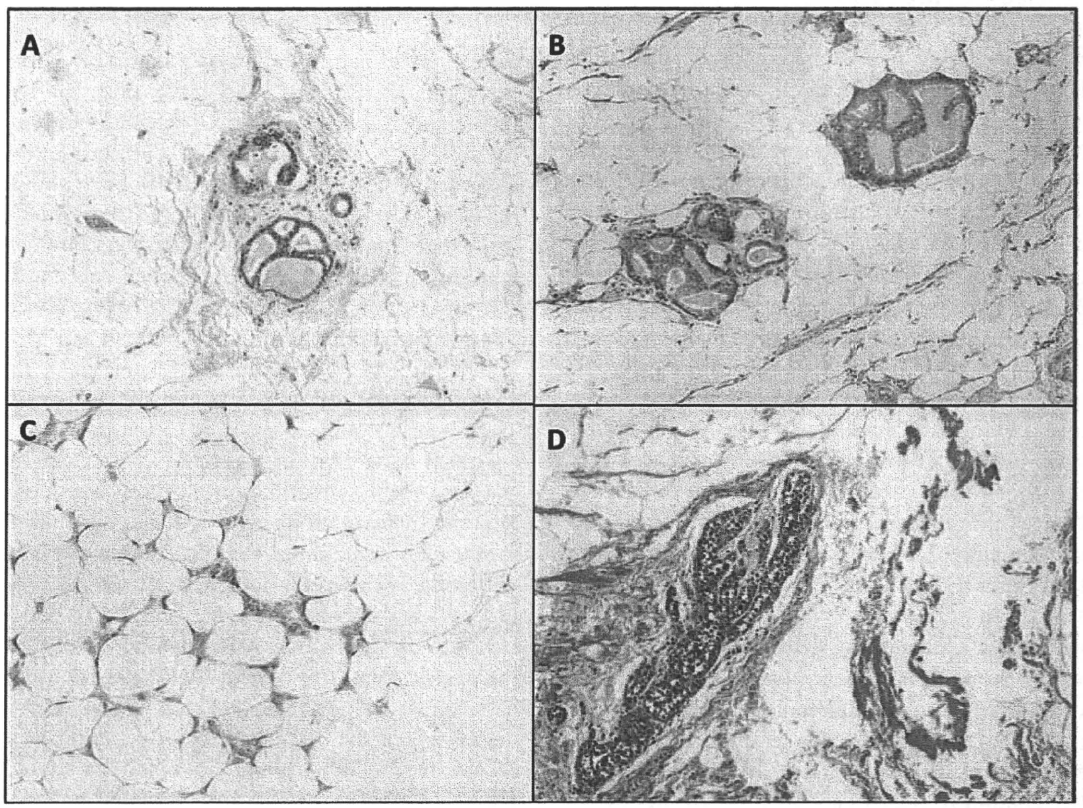

Figure 5. Representative illustrations of the carcinoma extensions which could not be detected by ultrasonography (US). (A) and (B) are low-grade intraductal components. (C) Is invasive lobular carcinoma extension and (D) is LCIS lesion.

Downloaded from jjco.oxfordjournals.org at Tohoku University on May 6, 2011

DISCUSSION

Previous studies demonstrated that the following ultrasonographic features such as oval or round shape, parallel orientation, circumscribed margins, abrupt interface, enhancement or absence of posterior acoustic features, absence of surrounding tissue alterations represented a benign breast lesion, whereas, irregular shape, non-parallel orientation, echogenic halo, posterior acoustic shadowing and abnormalities of the surrounding tissue regardless of echo pattern were considered to be consistent with a malignant lesion (5,18). It is also true that not all carcinomas fulfill these criteria and some do only partially (5). We therefore examined the details of preoperative US findings and compared these findings to their corresponding histopathological features of the surgical specimens.

It has been well known that circumscribed masses are usually detected in the cases in which carcinoma cells proliferated in both solid and expanded fashion. On the other hand, not circumscribed masses are detected in the cases in which carcinoma cells are arranged in cords, clusters and/or trabeculae, and/or are associated with mixed intraductal component and invasive areas. Halo is generally defined as one of back scattering in US (14). Reflection and scattering are detected and are considered to be caused by the structure which is heterogenous and smaller than sound wave, such as cellular tissue (14). Such opposite sound wave of incident element is generally defined as back scattering (19). Results of our present study demonstrated that halo was indeed characterized by the following histopathologic features, carcinoma cells infiltrated into fat tissue, mixed fat tissue, carcinoma cells and fibroblastic stroma.

Results of previous studies demonstrated that the degree of internal hypoechogenicity determines its sensitivity in predicting malignancy of the lesion (6,20,21). In addition, posterior shadowing has been also reported as one of the important US features suggestive of malignant nature of the lesions (6,20,22). It has been known that shadowing is provided by a highly cellular fibroblastic proliferation (2,14). This is the first study which demonstrated that anterior and posterior echoes were caused by the ratio of intratumoral carcinoma cells and fibroblastic stroma, and histological stromal characteristics. Results of our present study demonstrated that internal echoes and posterior echoes were defined by histopathological intratumoral construction. The acoustic characteristic impedance of the medium becomes larger, reflection subsequently becomes bigger and low internal echo and attenuation of posterior echo finally occur (14). In addition, low internal echo are also detected in the cases histopathologically associated with poor fibroblastic stroma, and carcinoma cells proliferating monotonously, solidly and confertusly. Internal and posterior acoustic shadowing is considered the direct result of US beam attenuation by the desmoplastic reaction to breast cancer (23). Results of our present study of histopathological correlation therefore demonstrated that internal low echoic masses represented the high ratio of fibroblastic stroma and the stroma in these lesions turned out to have marked degrees of interstitial collagenization or the tumors in which carcinoma cells proliferated monotonously, solidly and pushingly. In addition, attenuation of posterior echo was detected in the tumors histopathologically associated with hyperplasia of collagenized fibroblastic stroma. However, it is also true that increased cellularity in the mass with prominent large tumor nests and very little fibrous stroma demonstrated the accentuation or no change of the posterior echo. In addition, poor collagenized fibrous stroma exhibits high acoustic impedance. Histopathological intratumoral construction is important for internal and posterior echoes.

Results of our present study demonstrated that the concordance rate between the US findings and the histopathologic features was 91.6%. According to the comparison between the US findings in details and histopathologic features, we could reasonably postulate histological types from the US findings. Our results demonstrated that DCIS and ILC were lower concordance rates between estimated and actual histological types than the other types. As for DCIS, in some cases, intraductal components were gathered and formed nodule histopathologically. Therefore, the US findings of some DCIS cases were similar to some invasive carcinomas. On the other hand, some IDC tumors such as T1mic which have microinvasion 0.1 cm or less in greatest dimension were similar to DCIS because we proved that US is limited to detect the lesions with <1 mm in diameter. On the other hand, ILC is classified in the following types, classical pattern, solid pattern, alveolar pattern, pleomorphic lobular carcinoma and mixed type carcinoma (1). Therefore, US findings of ILC showed various features and US is limited in its ability to diagnose as ILC correctly. Previous study demonstrated that MR imaging has been shown to be particularly useful in the evaluation of ILC and DCIS (24). Our study also demonstrated the concordance rate of combined modalities was 96.8% (149 of 154 cases) with US, CT with CT skin marker and MRI. Especially, the concordance rate of ILC and DCIS were up to 57.1% (4 out of 7 cases) and 80.0% (8 out of the 10 cases), respectively. It is therefore very important to use a variety of imaging modalities for examining histological types of breast lesions.

Breast conservation therapy has become the treatment standard for the great majority of breast carcinoma (13,25). Several investigations reported the association of higher tumor recurrence rates with positive or close margins than with negative margins following breast-conserving therapy (25,26). It therefore becomes very important to precisely evaluate carcinoma extension preoperatively and determine the excision areas for performing breast-conserving surgery as accurate as possible (13). Results of our study clearly demonstrated the detection rate of carcinoma extension was 86.4% by US. Many tumors in which US could not appreciate carcinoma extension corresponded to DCIS following histopathological evaluations, especially DCIS associated with low-grade malignancy. In such low-grade malignant

Downloaded from jjco.oxfordjournals.org at Tohoku University on May 6, 2011

DCIS, intraductal components are very small, similar to non-pathologic breast ducts or lobes, the differentiation between low-grade malignant DCIS and non-pathologic breast tissue is generally defined only in cell or nuclear pleomorphism. In addition, such DCIS were rarely detected in stromal desmoplastic reaction. As for ILC, ILC can be insidious and difficult to detect on routine physical examination and/or imaging including US. Histopathologically, ILC is generally characterized by a proliferation of small cells, which lack cohesion and appear individually dispersed through a fibrous connective tissue or arranged in single file linear cords (1). There is often little host reaction or disturbance of the background architectures (1). In addition, this is the first study demonstrated that US is limited to detect the lesions with less than 1 mm in diameter. The results of this study demonstrated that the combined modalities such as US, CT and MRI increase the accuracy of detection from 86.4 to 93.8%. Therefore, it has become very important that a variety of imaging modalities has been used for examining tumor extension and multifocality in breast cancer patients.

CONCLUSION

We clarified the histopathological features of the breast lesions of the tumors in which carcinoma extension could not be preoperatively detected using US. The results of this study demonstrated correlation between histopathological and ultrasonographic findings of the breast lesions is cardinal for quality control or improving the quality of US.

Conflict of interest statement

None declared.

References

1. Tavassoli FA, Devilee P. World Health Organization Classification of Tumors. Tumor of the Breast and Females Genital Organs. Lyon: IARC Press.
2. *American College of Radiology Breast Imaging Reporting and Data System (BI-RADS), Ultrasound*, 4th edn. Reston, VA: ACR. http://www.acr.org/SecondaryMainMenuCategories/quality_safety/BIRADSAtlas/BIRADSAtlasexcerptedtext/BIRADSUltrasoundFirstEdition/ACRBIRADSUSLexiconClassificationFormDoc1.aspx (2 May 2010, date last accessed).
3. Tsunoda HS, Tohno E, Ueno E. Examination of effectiveness of breast cancer detection by modalities and age groups. *J Jpn Assoc Breast Cancer Screen* 1998;7:281–5.
4. Osako T, Takahashi K, Iwase T, Iijima K, Miyagi Y, Nishimura S, et al. Diagnostic ultrasonography and mammography for invasive and noninvasive breast cancer in women aged 30 to 39 years. *Breast Cancer* 2007;14:229–33.
5. Zonderland HM, Hermans J, Coerkamp EG. Ultrasound variables and their prognostic value in a population of 1103 patients with 272 breast cancers. *Eur Radiol* 2000;10:562–1568.
6. Chao TC, Lo YF, Chen SC, Chen MF. Prospective sonographic study of 3039 breast tumors. *J Ultrasound Med* 1999;18:363–70.
7. Ishida T, Furuta A, Moriya T, Ohuchi N. Pathological assessment of intraductal spread of carcinoma in relation to surgical margin state in breast-conserving surgery. *Jpn J Clin Oncol* 2003;33:61–166.
8. Ohuchi N. Breast-conserving surgery for invasive cancer: a principle based on segmental anatomy. *Tohoku J Exp Med* 1999;108:03–118.
9. Tsunoda-Shimizu H, Ueno E, Tohno E. Ultrasonographic evaluation for breast conservative therapy. *Jpn J Breast Cancer* 1996;11:649–55.
10. Kamio T, Kameoka S, Hamano K, Kimura T. Indication for breast conservative surgery by ultrasonography. *Jpn J Breast Cancer* 1996;11:656–64.
11. Amano G, Yajima M, Moroboshi Y, Kuriya Y, Ohuchi N. MRI accurately depicts underlying DCIS in a patient with Paget's disease of the breast without palpable mass and mammography findings. *Jpn J Clin Oncol* 2005;35:49–153.
12. Hata T, Takahashi H, Watanabe K, Takahashi M, Taguchi K, Itoh T, et al. Magnetic resonance imaging for preoperative evaluation of breast cancer: comparative study with mammography and ultrasonography. *J Am Coll Surg* 2004;198:90–197.
13. Harada-Shoji N, Yamada T, Ishida T, Amari M, Suzuki A, Moriya T, et al. Usefulness of lesion image mapping with multidetector-row helical computed tomography using a dedicated skin marker in breast-conserving surgery. *Eur Radiol* 2009;19:868–74.
14. Japan Association of Breast and Thyroid Sonology. *Guideline for Breast Ultrasound-Management and Diagnosis*, 2nd edn. Tokyo: Japanese 2008.
15. Sakamoto G, Inaji H, Akiyama F, Haga S, Hiraoka M, Inai K, et al. General rules for clinical and pathological recording of breast cancer 2005. *Breast Cancer* 2005;12(Suppl.): S1–27.
16. Rosen PP. *Rosen's Breast Pathology*, 3rd edn. Philadelphia, PA: Lippincott Williams & Wilkins, 2009.
17. Amano G, Ohuchi N, Ishibashi T, Ishida T, Amari M, et al. Correlation of three-dimensional magnetic resonance imaging with precise histopathological map concerning carcinoma extension in the breast. *Breast Cancer Res Treat* 2000;60:3–55.
18. Costantini M, Belli P, Ierardi C, Franceschini G, La Torre G, Bonomo L. Solid breast mass characterization: use of the sonographic BI-RADS classification. *Radiol med* 2007;112:877–94.
19. Koushi N. Basis of Ultrasound Diagnostic System and Technology. Tokyo: Japanese 2009.
20. Leucht WJ, Rade DR, Humbert KD. Diagnostic value of different interpretative criteria in real-time sonography of the breast. *Ultrasound Med Biol* 1988;14:59–73.
21. Jackson VP. Sonography of malignant breast disease. *Semin Ultrasound CT MR* 1989;10:119–31.
22. Harper AP, Kelly-Fry E, Noe JS, Bies JR, Jackson VP. Ultrasound in the evaluation of solid breast masses. *Radiology* 1983;146:731.
23. Kobayashi T. Diagnostic ultrasound in breast cancer: analysis of retro-tumorous echo patterns correlated with sonic attenuation by cancerous connective tissue. *JCU J Clin Ultrasound* 1979;7:471–9.
24. Lee CH. Problem solving MR imaging of the breast. *Radiol Clin N Am* 2004;42:919–34.
25. Singletary SE. Surgical margins in patients with early-stage breast cancer treated with breast conservation therapy. *Am J Surg* 2002;184:383–93.
26. Lindley R, Bulman A, Parsons P, Phillips R, Henry K, Ellis H. Histologic features predictive of an increased risk of early local recurrence of treatment of breast cancer by local tumour excision and radical radiotherapy. *Surgery* 1989;105:13–20.

Downloaded from jjco.oxfordjournals.org at Tohoku University on May 6, 2011

Cancer Science
The official journal of the Japanese Cancer Association

Immunolocalization of estrogen-producing and metabolizing enzymes in benign breast disease: Comparison with normal breast and breast carcinoma

Yoshie Sasaki,[1] Yasuhiro Miki,[2] Hisashi Hirakawa,[3] Yoshiaki Onodera,[2] Kiyoshi Takagi,[1] Jun-ichi Akahira,[2] Seijiro Honma,[4] Takanori Ishida,[5] Mika Watanabe,[6] Hironobu Sasano[2] and Takashi Suzuki[1,7]

Departments of [1]Pathology and Histotechnology; [2]Anatomic Pathology, Tohoku University Graduate School of Medicine, Sendai; [3]Department of Surgery, Tohoku Kosai Hospital, Sendai; [4]Research and Development Department, ASKA Pharma Medical Co., Ltd., Kanagawa; [5]Department of Surgical Oncology, Tohoku University Graduate School of Medicine, Sendai; [6]Department of Pathology, Tohoku University Hospital, Sendai, Japan

(Received April 22, 2010/Revised June 26, 2010/Accepted June 28, 2010/Accepted manuscript online July 7, 2010/Article first published online August 2, 2010)

It is well known that estrogens play important roles in the cell proliferation of breast carcinoma. Benign breast disease (BBD) contains a wide spectrum of diseases, and some are considered an important risk factor for subsequent breast carcinoma development. However, the significance of estrogens in BBD has remained largely unknown. Therefore, in this study, we examined tissue concentrations of estrogens and immunolocalization of estrogen-producing/metabolizing enzymes in BBD, and compared these findings with those in the normal breast and ductal carcinoma *in situ* (DCIS). Tissue concentration of estradiol in BBD (n = 9) was significantly (3.4-fold) higher than normal breast (n = 9) and nearly the same (0.7-fold) as in DCIS (n = 9). Immunoreactivity of estrogen sulfotransferase in BBD was significantly lower (n = 82) than normal breast (n = 28) but was not significantly different from DCIS (n = 28). Aromatase and steroid sulfatase immunoreactivities tended to be higher (P = 0.07) in BBD than in normal breast, and 17β-hydroxysteroid dehydrogenase type 1 immunoreactivity was significantly higher in BBD than normal breast in the postmenopausal tissues. Immunoreactivity of estrogen and progesterone receptors was also significantly higher in BBD than normal breast. These results suggest that tissue concentration of estradiol is increased in BBD at a level similar to DCIS, which is considered mainly due to loss of estrogen sulfotransferase expression. Increased local estradiol concentration in BBD due to aberrant expression of estrogen-producing/metabolizing enzymes may play important roles in the accumulation of estradiol-mediated growth and/or subsequent development of breast carcinoma. (*Cancer Sci* 2010; 101: 2286–2292)

Benign breast disease (BBD) is the most common disorder of the breast in women, and encompasses a wide variety of histological entities.[1,2] Some BBD are considered an important risk factor for subsequent development of breast carcinoma in the same patients. Among the histological subtypes of BBD, atypical ductal hyperplasia (ADH) has the highest (approximately 4-fold) risk of developing breast carcinoma, but patients with common proliferating BBD, such as fibroadenoma (FA), papilloma, sclerosing adenosis (SA), or usual ductal hyperplasia (UDH), are also known to be at increased (approximately 2-fold) risk of malignancy, although controversies have existed.[2–4]

Human breast tissue is a well-known estrogen target tissue. Biologically active estrogen, estradiol, contributes immensely to the growth of breast carcinoma, and endocrine therapy has been used in patients with breast carcinoma to inhibit intratumoral estrogen actions. Benign breast disease frequently expressed estrogen receptor (ER),[5–10] and women who had used postmenopausal hormonal supplementation were reported to be associated with an increased risk of BBD.[11,12] Treatment with an anti-estrogen tamoxifen significantly reduced the volume and cell proliferation activity of FA[13,14] and The National Surgical Adjuvant Breast Project Breast Cancer Prevention Trial showed that tamoxifen significantly reduced the risk of BBD, by approximately 28%.[15] These findings all suggest the importance of estrogens in the development and/or progression of BBD.

In breast carcinoma, estradiol is locally produced from circulating inactive steroids by estrogen-producing enzymes, such as aromatase (conversion from androstenedione to estrone, or testosterone to estradiol), steroid sulfatase (STS; hydrolysis of estrone sulfate to estrone) and 17β-hydroxysteroid dehydrogenase type 1 (17βHSD1; reduction of estrone to estradiol).[16] Estrogens are also inversely inactivated by estrogen sulfotransferase (EST; sulfonation of estrogen to estrogen sulfate)[17] or 17βHSD2 (oxidation of estradiol to estrone).[16] Pasqualini *et al.*[18] reported that estradiol concentration and STS activity was significantly higher in FA than the corresponding normal human breast tissue, and Ariga *et al.*[8] reported immunolocalization of 17βHSD1 and 17βHSD2 in UDH and ADH. However, other information regarding estrogen concentration or estrogen-producing/metabolizing enzymes is unknown in BBD, and the significance of estrogens remains largely uncharacterized in BBD. Therefore, in our present study, we examined the tissue concentration of estrogens and immunolocalization of estrogen-producing/metabolizing enzymes in BBD, and compared these findings with those in normal breast and ductal carcinoma *in situ* (DCIS), an early stage of breast carcinoma, in order to analyze the status of *in situ* estrogen production.

Materials and Methods

Patients and tissues. Snap-frozen specimens of nine BBD (FA [n = 7] and SA [n = 2]), and nine pure DCIS tissues were used in order to examine the tissue concentration of estrogens. These specimens were obtained from nine premenopausal female patients (aged 23–48 years for BBD and 33–49 years for DCIS) who underwent surgical treatment from 2001 to 2008 in the Departments of Surgery at Tohoku University Hospital and Tohoku Kosai Hospital (Sendai, Japan). Snap-frozen specimens of nine breast tissues, which were distant from the invasive breast carcinoma associated with no significant histopathological

[7]To whom correspondence should be addressed.
E-mail: t-suzuki@patholo2.med.tohoku.ac.jp

doi: 10.1111/j.1349-7006.2010.01673.x
© 2010 Japanese Cancer Association

abnormalities, were also used in this study as normal breast tissues. These specimens were all obtained from premenopausal patients (aged 41–50 years) who had invasive breast carcinoma and underwent mastectomy in the Department of Surgery at Tohoku Kosai Hospital. All of the specimens were stored at −80°C, and histology was confirmed before estrogen extraction using frozen tissue sections.

Eighty-two BBD lesions, comprising FA (n = 29), papilloma (n = 20), SA (n = 16), and UDH (n = 17), were obtained from 68 pure BBD patients by surgical excision between 1998 and 2007 in the Department of Surgery, Tohoku University Hospital. Examination of atypical papilloma or ADH was not available in this study. The mean age of BBD patients was 43 years (range, 16–68 years). Among these patients, the breast tissue associated with no significant histopathological abnormalities was available for examination in 28 cases. They were used as normal breast tissue in this portion of the study. Twenty-eight specimens of pure DCIS were obtained by surgical excision between 1998 and 2007 in the Department of Surgery, Tohoku University Hospital. The mean age of the patients was 52 years (range, 30–77 years). All the specimens were fixed with 10% formalin and embedded in paraffin wax. The menopausal status of patients was retrieved from patient charts. The number of tissues obtained from postmenopausal patients (at least 1 year after menopause, aged more than 50 years) was eight in normal breast, 16 in BBD, and 16 in DCIS.

Research protocols for this study were approved by the Ethics Committee at Tohoku University School of Medicine (No. 2008–382).

Liquid chromatography/electrospray tandem mass spectrometry (LC-MS/MS). Concentrations of estrone and estradiol were measured by LC-MS/MS analysis in ASKA Pharma Medical (Kawasaki, Japan), as described previously.[19] Briefly, breast tissue specimens (~50 mg for each sample) were homogenized in 1 mL distilled water, and steroid fraction was extracted with diethyl ether. After application to a Bond Elut C18 column (Varian, Inc., Palo Alto, CA, USA), steroid derivatives were eluted with 80% acetonitrile solution.

An API-5000 triple stage quadrupole mass spectrometer equipped with an electrospray ionization (ESI) ion source (Applied Biosystems, Foster City, CA, USA) and a Shimadzu HPLC system (Shimadzu, Kyoto, Japan) were used in our study. The chromatographic separation was carried out on Cadenza CD-C18 column (150 mm × 3 mm i.d., 3 μm; Imtakt, Kyoto, Japan) at 40°C. The mobile phase, consisting of CH3CN–CH3OH (50:50, v/v) (Solvent A) and 0.1% HCOOH (Solvent B), was used with a gradient elution of A:B = 60:40–90:10 (0–5.5 min), 90:10–100:0 (5.5–7.5 min), 100:0 (7.5–8.5 min) and 40:60 (8.5–10 min) at a flow rate of 0.4 mL/min. ESI/MS conditions were as follows: spray voltage, 3300 V; collision gas, nitrogen, 1.5 psi (gas pressure); curtain gas nitrogen, 11 psi; ion source temperature, 600°C; and ion polarity positive.

The derived estrone and estradiol were determined using product ions (m/z 157 and 264, respectively) produced from their individual protonated molecular ions. The limit of quantification was 4 fmol/g for estrone, and 2 fmol/g for estradiol.

Immunohistochemistry. The characteristics of primary antibodies for aromatase,[20] STS,[21] and EST[22] were described previously. The primary antibodies for aromatase and STS were kindly provided by Dr. Dean B. Evans (Novartis Institutes for BioMedical Research Basel, Oncology Research, Basel, Switzerland) and Dr. Taisuke Nakata (Strategic Product Planning Department, Kyowa Hakko Kirin, Tokyo, Japan), respectively. Monoclonal antibody for 17βHSD1 (EP1682Y) and polyclonal antibody for 17βHSD2 (10978-1-AP) were purchased from Epitomics (Burlingame, CA, USA) and Proteintech Group (Chicago, IL, USA), respectively. Monoclonal antibodies for ER (ER1D5) and progesterone receptor (PR; MAB429) were purchased from Immunotech (Marseille, France) and Chemicon (Temecula, CA, USA). A Histofine kit (Nichirei, Tokyo, Japan), which uses the streptavidin–biotin amplification method, was used for immunohistochemistry in this study. Antigen retrieval was carried out by heating the slides in an autoclave at 120°C for 5 min for ER, PR, and EST immunostaining, and by heating the slides in a microwave at for 20 min for 17βHSD1 immunostaining. The dilution of primary antibodies used in this study was as follows: aromatase, 1/3000; STS, 1/200; 17βHSD1, 1/400; EST, 1/100; 17βHSD2, 1/200; ER, 1/50; and PR, 1/30. The antigen–antibody complex was visualized with 3.3′-diaminobenzidine solution (1 mM 3.3′-diaminobenzidine, 50 mM Tris–HCl buffer (pH 7.6), and 0.006% H_2O_2) and counterstained with hematoxylin.

Immunoreactivity of the estrogen-producing/metabolizing enzyme was detected in the cytoplasm of epithelial or carcinoma cells, and cases that had more than 10% positive cells were considered positive.[23] Immunoreactivity of ER and PR was detected in the nucleus of epithelial or carcinoma cells. These immunoreactivities were evaluated in more than 1000 epithelial or carcinoma cells for each case and subsequently the percentage of immunoreactivity, the labeling index (LI), was determined.

Statistical analysis. The statistical analyses between two groups were carried out using the Mann–Whitney U-test and cross-table using the χ^2-test. Analyses among groups were carried out using Kruskal–Wallis test and cross-table using the χ^2-test. P-values <0.05 were considered significant. The relative ratio between two groups was evaluated by their median values.

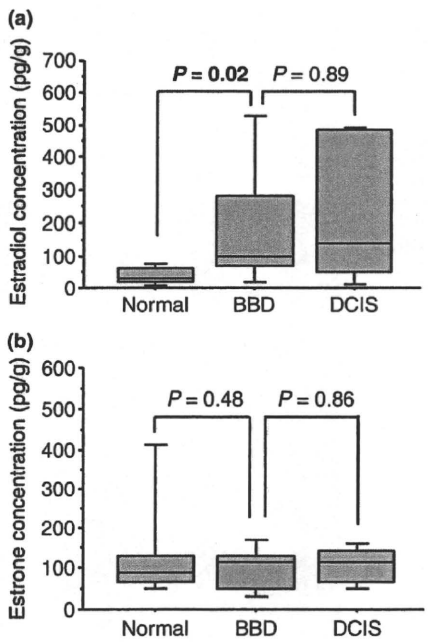

Fig. 1. Tissue concentrations of estradiol (a) and estrone (b) in benign breast disease (BBD). Data are represented as box and whisker plots. The median value is represented by a horizontal line in each box. The 75th (upper margin) and 25th (lower margin) percentiles of the values are shown. The upper and lower bars indicate the 90th and 10th percentiles, respectively. Statistical analysis was carried out using the Mann–Whitney U-test. P-values <0.05 were considered significant, and are indicated in bold. DCIS, ductal carcinoma *in situ*; normal, breast tissue with no significant pathological abnormalities.

© 2010 Japanese Cancer Association

Results

Tissue concentration of estrogens in BBD. We first examined tissue concentration of estrogens in normal breast, proliferating BBD, and DCIS tissues using LC-MS/MS. The median (minimum–maximum) value of tissue concentration of estradiol was 29 (4–82) pg/g in normal breast, 98 (3–674) pg/g in BBD, and 139 (12–494) pg/g in DCIS (Fig. 1a). The median value of estradiol in BBD was significantly ($P = 0.02$ and 3.4-fold) higher than that in normal breast, but it was similar ($P = 0.89$ and 0.7-fold) to that in DCIS. However, the median (minimum–maximum) value of estrone concentration in normal breast, BBD, and DCIS was 86 (46–560), 114 (20–195), and 113 (40–159) pg/g, respectively (Fig. 1b).

Immunolocalization of estrogen-producing/metabolizing enzymes in BBD. We then immunolocalized estrogen-producing (aromatase, STS, and 17βHSD1) and metabolizing (EST and 17βHSD2) enzymes in normal breast, proliferating BBD, and DCIS cases. Aromatase immunoreactivity was negative in the normal breast (Fig. 2a), but was focally detected in the epithelial cells in 9 out of 82 (11%) BBD lesions (Fig. 2b,c). Aromatase immunoreactivity was positive in the carcinoma cells in 13 out of 28 (46%) DCIS cases, and was also detected in some intratumoral stromal cells as reported previously.[23] Steroid sulfatase immunoreactivity was negative in normal breast (Fig. 2d) except for 1 (4%) case; the enzyme was focally detected in epithelial cells in 14 out of 82 (17%) BBD (Fig. 2e,f). Steroid sulfatase immunoreactivity was positive in carcinoma cells in 10 out of 28 (36%) DCIS cases. 17βHSD1 immunoreactivity was detected in epithelial cells or carcinoma cells in 8 out of 28 (29%) normal breasts, 32 out of 82 (39%) BBD, and 17 out of 28 (61%) DCIS cases. Both STS and 17βHSD1 immunoreactivity was not detected in stromal cells of any of the specimens examined in this study. Estrogen sulfotransferase immunoreactivity was detected in the epithelial cells in 25 out of 28 (89%) normal breasts (Fig. 2g), but was positive in only 40 out of 82 (49%) BBD (Fig. 2h,i) and 14 out of 28 (50%) DCIS cases. 17βHSD2 immunoreactivity was detected in epithelial cells or carcinoma cells in 5 out of 28 (18%) normal breasts, 13 out of 82 (16%) BBD, and 3 out of 28 (11%) DCIS cases, respectively.

Association of immunoreactivity of these enzymes between BBD and normal breast or DCIS is summarized in Table 1. Immunoreactivity of aromatase and STS was more frequent in BBD than normal breast, although the association did not reach statistical significance ($P = 0.07$) (Table 1A). Immunoreactivity of aromatase, STS, and 17βHSD1 was significantly higher in DCIS than BBD ($P < 0.0001$ in aromatase; $P = 0.04$ in STS; $P = 0.046$ in 17βHSD1). However, EST immunoreactivity in BBD was significantly ($P = 0.0004$) lower than in normal breast, but was similar to that in DCIS ($P = 0.91$) (Table 1B). No significant association of 17βHSD2 immunoreactivity was detected between BBD and normal breast ($P = 0.81$) or DCIS ($P = 0.51$) in this study.

Statistical association of the estrogen-producing/metabolizing enzyme immunoreactivity between BBD and normal breast or DCIS according to the menopausal status is summarized in Table 2. Aromatase immunoreactivity was significantly ($P = 0.003$) higher in DCIS than BBD in premenopausal tissues, and a similar tendency ($P = 0.06$) was also detected in postmenopausal cases. 17βHSD1 immunoreactivity was significantly

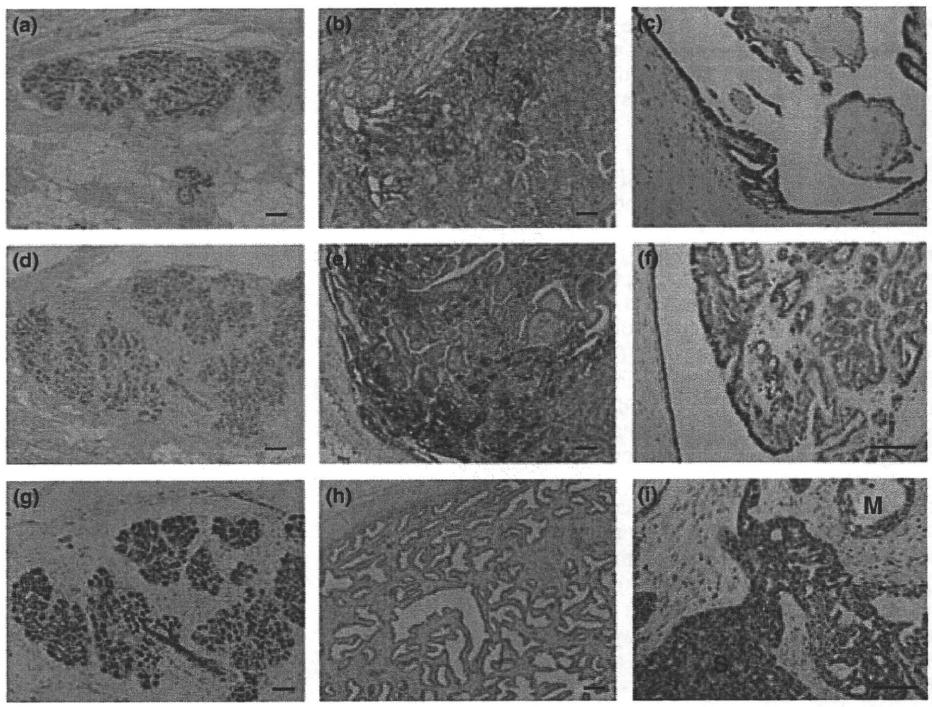

Fig. 2. Representative illustrations of immunohistochemistry for estrogen-producing/metabolizing enzymes in benign breast disease. Aromatase immunoreactivity was negative in normal breast (a), but was detected in the epithelium of the papilloma (b,c). Aromatase immunolocalization was observed in a part of the hyperplastic (b) or simple epithelium in the same case (c). Steroid sulfatase immunoreactivity was not detected in the normal breast (d), but it was positive in the epithelium of the papilloma (e,f). Steroid sulfatase immunoreactivity was observed in a part of the hyperplastic (e) or simple epithelium in the same case (f). Estrogen sulfotransferase immunoreactivity was detected in normal epithelial cells (g), but was negative in fibroadenoma (h). Estrogen sulfotransferase immunoreactivity was positive in various degree of hyperplastic epithelium in usual ductal hyperplasia (i). M, mild hyperplasia component (three to four cell layers thick); S, severe (or florid) hyperplasia component (solid duct hyperplasia). Bar = 100 μm.

doi: 10.1111/j.1349-7006.2010.01673.x
© 2010 Japanese Cancer Association

Table 1. Immunoreactivity for (A) estrogen-producing enzymes, (B) estrogen-metabolizing enzymes in normal breast, benign breast disease (BBD), and ductal carcinoma *in situ* (DCIS)

Enzymes	Immunoreactivity	Normal (n = 28)	BBD (n = 82)	DCIS (n = 28)	*P*-value	
					Normal *vs* BBD	BBD *vs* DCIS
A						
Aromatase	+	0 (0%)	9 (11%)	13 (46%)		
	−	28 (100%)	73 (89%)	15 (54%)	0.07	**<0.0001**
STS	+	1 (4%)	14 (17%)	10 (36%)		
	−	27 (96%)	68 (83%)	18 (64%)	0.07	**0.0400**
17βHSD1	+	8 (29%)	32 (39%)	17 (61%)		
	−	20 (71%)	50 (61%)	15 (39%)	0.32	**0.0460**
B						
EST	+	25 (89%)	40 (49%)	14 (50%)		
	−	3 (11%)	42 (51%)	14 (50%)	**0.0004**	0.9100
17βHSD2	+	5 (18%)	13 (16%)	3 (11%)		
	−	23 (82%)	69 (84%)	25 (89%)	0.8100	0.5100

Data are presented as the number of cases and percentage in each histological group. *P*-values were evaluated by a cross-table using the χ^2-test between two histological groups. *P*-values <0.05 were considered significant, and are shown in bold. EST, estrogen sulfotransferase; normal, breast tissue showing no significant pathological abnormalities; STS, steroid sulfatase; 17βHSD1, 17β-hydroxysteroid dehydrogenase type 1.

Table 2. Statistical association of immunoreactivity of estrogen-producing/metabolizing enzymes between benign breast disease (BBD) and normal breast or ductal carcinoma *in situ* (DCIS) according to menopausal status

Enzymes	Premenopausal tissues		Postmenopausal tissues	
	Normal (n = 20) *vs* BBD (n = 66)	BBD (n = 66) *vs* DCIS (n = 20)	Normal (n = 8) *vs* BBD (n = 16)	BBD (n = 16) *vs* DCIS (n = 16)
Estrogen-producing enzymes				
Aromatase	0.16	**0.003**	0.19	0.06
STS	0.19	0.180	0.19	0.24
17βHSD1	0.98	0.180	**0.02**	>0.99
Estrogen-metabolizing enzymes				
EST	**0.01**	0.73	**0.01**	>0.99
17βHSD2	0.45	0.43	0.37	**0.01**

Data are presented as *P*-values, evaluated by a cross-table using the χ^2-test between two histological groups. *P*-values <0.05 were considered significant, and are shown in bold. EST, estrogen sulfotransferase; normal, breast tissue showing no significant pathological abnormalities; STS, steroid sulfatase; 17βHSD1, 17β-hydroxysteroid dehydrogenase type 1.

(P = 0.02) higher in BBD than normal breast in postmenopausal tissues. Statistical association of EST immunoreactivity was detected between BBD and normal breast regardless of the menopausal status of subjects examined (P = 0.01). 17βHSD2 immunoreactivity was significantly (P = 0.01) lower in DCIS than BBD in the postmenopausal tissues.

Estrogen receptor and progesterone receptor immunoreactivity in BBD. Nuclear ER immunoreactivity was detected in the epithelial cells or carcinoma cells of normal breast, BBD (Fig. 3a), and DCIS. Estrogen receptor LI was significantly (P < 0.0001 and 2.8-fold) higher in BBD than that in the normal breast, and it was significantly (P < 0.0001 and 3.3-fold) higher in DCIS than BBD (Fig. 3b). Progesterone receptor immunoreactivity was also detected in epithelial cells or carcinoma cells of normal breast, BBD (Fig. 3c), and DCIS. Progesterone receptor LI in BBD was significantly (P < 0.0001 and 6.5-fold) higher than that in normal breast, but was not significantly different (P = 0.39 and 1.0-fold) from that in DCIS (Fig. 3d). Progesterone receptor LI was positively associated (P = 0.002 and r = 0.34) with ER LI in 82 BBD tissues examined.

Immunohistochemical features of enzymes in BBD according to histological types. As summarized in Table 3, no significant differences of immunoreactivity for aromatase, STS, 17βHSD1, EST, 17βHSD2, ER, or PR were detected among four different histological subtypes of proliferating BBD examined in this study. It is known that BBD includes variable histological appearances.[24] However, by immunohistochemical observations, we could not find an association between such a histological appearance and immunoreactivity of estrogen-producing/metabolizing enzymes. For instances, immunoreactivity of aromatase (Fig. 2b,c) and STS (Fig. 2e,f) was focally detected in the papilloma regardless of the degree of epithelial hyperplasia, and EST immunoreactivity was observed in various thicknesses of the epithelium in UDH (Fig. 2i).

When we examined an association among immunoreactivity of estrogen-producing/metabolizing enzymes in 82 BBD tissues, positive association was detected between aromatase and 17βHSD1 (P = 0.03), aromatase and 17βHSD2 (P = 0.003), and STS and 17βHSD1 (P = 0.02). However, these immunoreactivities were not necessarily colocalized in the same lesions or constitutive cells of the one lesion within a case by immunohistochemical observations.

Immunohistochemical features of enzymes in DCIS. Associations between immunoreactivity of estrogen-producing/metabolizing enzymes and clinicopathological parameters in the 28 DCIS cases are summarized in Table 4. Among these enzymes, immunoreactivity for EST and 17βHSD2 was inversely associated with ER LI (P = 0.01 and P = 0.04, respectively). Immunoreactivity for STS tended to be positively associated with Van Nuys classification (P = 0.051) in this study, and a significant positive association between these was previously reported in 83 DCIS cases.[23] No significant association was detected among the immunoreactivity of these enzymes in DCIS cases examined.

Discussion

In our present study, tissue estradiol concentration in BBD was significantly (P = 0.02 and 3.4-fold) higher than that in normal breast, and was similar to that in DCIS. Pasqualini *et al.*[18] reported that estradiol concentration of FA was three times higher than the corresponding normal breast in premenopausal women, which is in good agreement with results of our present study. Estradiol concentration in normal breast tissue was low regardless of the menopausal status, although it is very high in

© 2010 Japanese Cancer Association

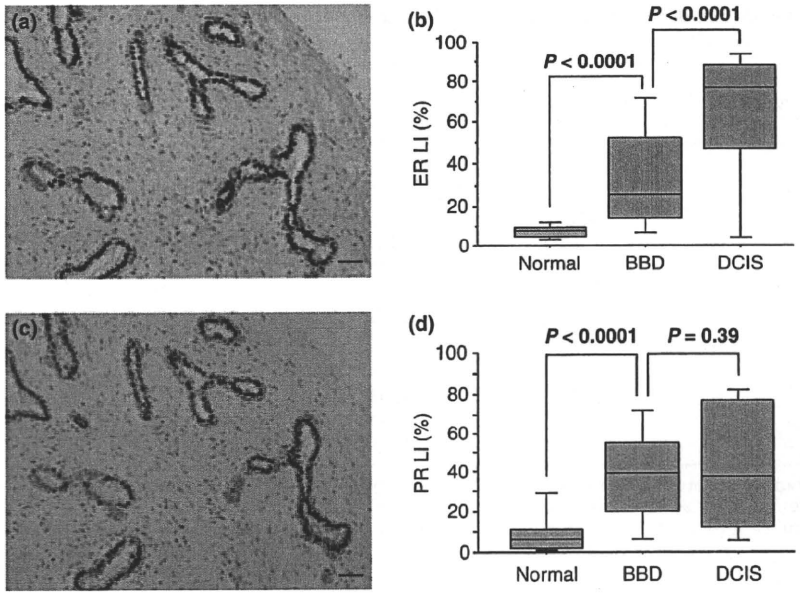

Fig. 3. Estrogen receptor (ER) and progesterone receptor (PR) immunoreactivity in benign breast disease (BBD). (a,c) Estrogen receptor (a) and progesterone receptor (c) immunoreactivity was detected in the nuclei of epithelial cells in this case of fibroadenoma. Images show the same area. Bar = 100 μm. (b,d) Association of ER (b) and PR (d) labeling indexes (LI) between BBD and normal breast or ductal carcinoma *in situ* (DCIS). Data are represented as box and whisker plots. The statistical analysis was carried out using the Mann–Whitney *U*-test. *P*-values <0.05 were considered significant, and are shown in bold.

Table 3. Immunoreactivity of estrogen-producing/metabolizing enzymes and sex hormone receptors in benign breast disease (BBD) according to histological types

Enzymes	Immunoreactivity	FA (n = 29)	Papilloma (n = 20)	SA (n = 16)	UDH (n = 17)	*P*-value
Estrogen-producing enzymes						
Aromatase	+	2 (7%)	3 (15%)	3 (19%)	1 (6%)	
	–	27 (93%)	17 (85%)	13 (81%)	16 (94%)	0.52
STS	+	6 (21%)	4 (20%)	3 (19%)	1 (6%)	
	–	23 (79%)	16 (80%)	13 (81%)	16 (94%)	0.59
17βHSD1	+	12 (41%)	10 (50%)	5 (31%)	5 (29%)	
	–	17 (59%)	10 (50%)	11 (69%)	12 (71%)	0.54
Estrogen-metabolizing enzymes						
EST	+	18 (62%)	9 (45%)	7 (44%)	8 (47%)	
	–	11 (38%)	11 (55%)	9 (56%)	9 (53%)	0.54
17βHSD2	+	2 (7%)	4 (20%)	3 (19%)	4 (24%)	
	–	27 (93%)	16 (80%)	13 (71%)	13 (76%)	0.41
Sex hormone receptors						
ER LI†	NA	31 (0–74)	23 (4–88)	21 (4–89)	42 (0–82)	0.65
PR LI†	NA	45 (1–86)	24 (0–82)	28 (0–77)	44 (0–82)	0.11

†Data represent median (minimum–maximum), and *P*-values were evaluated by the Kruskal–Wallis test. Other values are presented as the number of cases and percentage in each histological group, and *P*-values were evaluated by a cross-table using the χ^2-test. ER, estrogen receptor; EST, estrogen sulfotransferase; FA, fibroadenoma; NA, not applicable; normal, breast tissue showing no significant pathological abnormalities; PR, progesterone receptor; SA, sclerosing adenosis; STS, steroid sulfatase; UDH, usual ductal hyperplasia; 17βHSD1, 17β-hydroxysteroid dehydrogenase type 1.

plasma before menopause.[25] However, the estradiol concentration was fivefold higher in invasive breast carcinoma tissue than plasma in premenopausal women,[26] and intratumoral estradiol level in DCIS was nearly comparable to that in invasive breast carcinoma.[23] Therefore, these data suggest that estradiol is predominantly metabolized in normal breast tissue, but its concentration is significantly increased in the proliferating BBD at a level comparable with that of breast carcinoma.

Among the enzymes examined in this study, statistically significant association was detected between normal breast and BBD only in the cases of EST (Table 1), and EST immunoreactivity was significantly (P = 0.004) lower in BBD than normal breast. Estrogen sulfotransferase is the only sulfotransferase that displays affinity for estradiol in a physiological concentration range, and the sulfating activity for estradiol was stronger than that for estrone.[17,27,28] Estrogen sulfotransferase is expressed

doi: 10.1111/j.1349-7006.2010.01673.x
© 2010 Japanese Cancer Association

Table 4. Statistical association between immunoreactivity of estrogen-producing/metabolizing enzymes and clinicopathological parameters in 28 cases of ductal carcinoma *in situ*

Enzymes	Patient age	Menopausal status	Van Nuys classification	ER LI	PR LI
Estrogen-producing enzymes					
Aromatase	0.91	0.95	0.370	0.17	0.56
STS	0.58	0.99	0.051	0.25	0.98
17βHSD1	0.08	0.16	0.690	0.16	0.12
Estrogen-metabolizing enzymes					
EST	0.25	0.52	0.610	**0.01**	0.27
17βHSD2	0.37	0.71	0.250	**0.04**	0.37

Data are presented as *P*-values, evaluated by a cross-table using the χ^2-test or the Mann–Whitney *U*-test. *P*-values <0.05 were considered significant, and are shown in bold. 17βHSD1, 17β-hydroxysteroid dehydrogenase type 1; ER, estrogen receptor; EST, estrogen sulfotransferase; LI, labeling index; PR, progesterone receptor; STS, steroid sulfatase.

in a wide variety of human tissues including breast, and is considered to be involved in protecting peripheral tissues from circulating excessive estrogenic effects.[22,29] Estrogen sulfotransferase immunoreactivity in breast carcinoma was frequently decreased compared to that in normal breast tissue, and was also shown to be inversely correlated with the tumor size or lymph node status.[22] Falany *et al.*[30] reported that MCF-7 breast carcinoma cells transfected with EST possessed EST at levels similar to normal human mammary epithelial cells, and these cells were actually associated with much lower estradiol-stimulated cell proliferation than control MCF-7 cells that do not express EST. Moreover, Fu *et al.*[31] very recently examined EST mRNA expression in an MCF-10A-derived lineage cell culture model, and reported that EST was abundantly expressed in MCF-10A and preneoplastic MCF-10AT1 cell lines, but was also markedly repressed in neoplastic MCF-10A-derived cell lines as well as in MCF-7 cells. These results all suggest that the loss of EST expression results in the increased local estradiol level in BBD by reducing its metabolism. Thus, EST is a possible key regulator of the estradiol concentration in BBD.

A great majority of BBD is well known to occur in premenopausal women,[1,32–34] which may be partly explained by decreased EST expression in BBD, as indicated in our present study. However, it is also true that some cases of BBD arise after menopause when serum estradiol level is negligible. In our present study, the immunoreactivity of aromatase and STS tended to be higher in BBD than normal breast, although *P* values did not reach statistical significance ($P = 0.07$). 17βHSD1 immunoreactivity was also significantly higher in BBD than normal breast in postmenopausal tissues. Pasqualini *et al.*[18] reported that STS activity in BBD was significantly higher than in corresponding normal breast tissue. 17βHSD1 immunoreactivity was also shown to be progressively increased according to UDH, ADH, and DCIS,[8] and Miyoshi *et al.*[35] reported that 17βHSD1 mRNA levels in invasive breast carcinoma were significantly higher in postmenopausal than in premenopausal tissue, suggesting the importance of 17βHSD1 associated with increased estradiol levels, especially in postmenopausal patients. Therefore, expression of estrogen-producing enzymes, such as aromatase, STS, and 17βHSD1, may also contribute to an increment of estradiol concentration in BBD.

In our study, ER and PR immunoreactivity was significantly higher in proliferating BBD than normal breast. Previous reports also indicated that ER and PR expression was increased in BBD compared to normal breast at both mRNA and protein levels.[5–7,9,10,36,37] Results of our present studies are consistent with these results. In addition, our present study also showed significant ($P = 0.002$ and $r = 0.34$) positive association between ER and PR immunoreactivity in BBD. Progesterone receptor expression is mainly regulated by estradiol through ER, and PR immunoreactivity in general reflects functional estrogen actions in breast carcinoma.[38,39] Cell proliferation activity of ER-positive cells was higher in BBD than normal breast.[9,36] As the immunoreactivity of estrogen-producing/metabolizing enzymes and sex hormone receptors was not significantly different among the histological types of proliferative BBD, as shown in Table 3, increased estrogen actions are postulated to be mainly associated with the progression, rather than the morphogenesis or pathogenesis, of the BBD lesion. In addition, proliferating BBD represents a risk factor for breast carcinoma,[2–4] and Shekhar *et al.*[40] showed that estradiol treatment frequently resulted in atypical hyperplasia, carcinoma *in situ*, and invasive carcinoma from proliferative BBD using an MCF-10AT xenograft model. Therefore, an increment of estradiol level in BBD due to aberrant expression of estrogen-producing/metabolizing enzymes may play an important role in accumulation of estradiol-mediated growth and subsequent development of breast carcinoma in BBD. Further investigations are warranted to clarify this issue.

Acknowledgments

We appreciate the skillful technical assistance of Ms. Miwako Kikuchi (Department of Pathology and Histotechnology, Tohoku University Graduate School of Medicine), and Ms. Miki Mori and Mr. Katsuhiko Ono (both Department of Anatomic Pathology and Tohoku University Graduate School of Medicine).

References

1 Devitt JE. Clinical benign disorders of the breast and carcinoma of the breast. *Surg Gynecol Obstet* 1981; **152**: 437–40.
2 Hartmann LC, Sellers TA, Frost MH *et al.* Benign breast disease and the risk of breast cancer. *N Engl J Med* 2005; **353**: 229–37.
3 Dupont WD, Page DL. Risk factors for breast cancer in women with proliferative breast disease. *N Engl J Med* 1985; **312**: 146–51.
4 Carter CL, Corle DK, Micozzi MS, Schatzkin A, Taylor PR. A prospective study of the development of breast cancer in 16,692 women with benign breast disease. *Am J Epidemiol* 1988; **128**: 467–77.
5 Allegra JC, Lippman ME, Green L *et al.* Estrogen receptor values in patients with benign breast disease. *Cancer* 1979; **44**: 228–31.
6 Jacquemier JD, Rolland PH, Vague D, Lieutaud R, Spitalier JM, Martin PM. Relationships between steroid receptor and epithelial cell proliferation in benign fibrocystic disease of the breast. *Cancer* 1982; **49**: 2534–6.
7 Tóth J, De Sombre ER, Greene GL. Immunohistochemical analysis of estrogen and progesterone receptors in benign breast diseases. *Zentralbl Pathol* 1991; **137**: 227–32.
8 Ariga N, Moriya T, Suzuki T *et al.* 17 beta-Hydroxysteroid dehydrogenase type 1 and type 2 in ductal carcinoma *in situ* and intraductal proliferative lesions of the human breast. *Anticancer Res* 2000; **20**: 1101–8.
9 Shoker BS, Jarvis C, Clarke RB *et al.* Abnormal regulation of the oestrogen receptor in benign breast lesions. *J Clin Pathol* 2000; **53**: 778–83.
10 Cericatto R, Pozzobon A, Morsch DM, Menke CH, Brum IS, Spritzer PM. Estrogen receptor-alpha, bcl-2 and c-myc gene expression in fibroadenomas and adjacent normal breast: association with nodule size, hormonal and reproductive features. *Steroids* 2005; **70**: 153–60.
11 Cui Y, Page DL, Lane DS, Rohan TE. Menstrual and reproductive history, postmenopausal hormone use, and risk of benign proliferative epithelial disorders of the breast: a cohort study. *Breast Cancer Res Treat* 2009; **114**: 113–20.
12 Rohan TE, Negassa A, Chlebowski RT *et al.* Conjugated equine estrogen and risk of benign proliferative breast disease: a randomized controlled trial. *J Natl Cancer Inst* 2008; **100**: 563–71.
13 Viviani RS, Gebrim LH, Baracat EC, De Lima GR. Evaluation of the ultrasonographic volume of breast fibroadenomas in women treated with tamoxifen. *Minerva Ginecol* 2002; **54**: 531–5.

© 2010 Japanese Cancer Association